NASA Technical Paper 1114

Thermal Performance of Gaseous-Helium-Purged Tank-Mounted Multilayer Insulation System During Ground-Hold and Space-Hold Thermal Cycling and Exposure to Water Vapor

Irving E. Sumner

AUGUST 1978

NASA

NASA Technical Paper 1114

Thermal Performance of Gaseous-Helium-Purged Tank-Mounted Multilayer Insulation System During Ground-Hold and Space-Hold Thermal Cycling and Exposure to Water Vapor

Irving E. Sumner
Lewis Research Center
Cleveland, Ohio

National Aeronautics
and Space Administration

**Scientific and Technical
Information Office**

1978

THERMAL PERFORMANCE OF GASEOUS-HELIUM-PURGED TANK-MOUNTED MULTILAYER INSULATION SYSTEM DURING GROUND-HOLD AND SPACE-HOLD THERMAL CYCLING AND EXPOSURE TO WATER VAPOR

by Irving E. Sumner

Lewis Research Center

SUMMARY

An experimental investigation was conducted to determine (1) the ground-hold and space-hold thermal performance of a multilayer insulation (MLI) system mounted on a spherical, liquid-hydrogen propellant tank and (2) the degradation to the space-hold thermal performance of the MLI system that occurred as a result of both thermal cycling and moisture introduced into the insulation panels. The propellant tank had a 1.39-meter (4.57-ft) diameter. The MLI consisted of two blankets of insulation; each blanket contained 15 double-aluminized Mylar radiation shields alternated with 16 double silk net spacers. A laminated aluminized Mylar and Dacron scrim cover sheet was applied to each side of each blanket.

Nineteen tests simulating basic cryogenic spacecraft thermal (environmental) conditions were conducted. Each thermal cycle typically included a gaseous-helium purge of the MLI, a liquid-hydrogen fill and ground-hold condition, a vacuum chamber pumpdown and a vacuum space-hold condition, and a repressurization of the vacuum chamber and insulation system back to a 1-atmosphere pressure. Prior to each of the last seven thermal cycle tests, water vapor was introduced into the vacuum chamber for varying periods of time to establish the resulting effect on the MLI space-hold thermal performance.

Initial baseline space-hold and ground-hold heat inputs of 7.18 and 3845 watts (24.5 and 13 130 Btu/hr), respectively, were measured. There was no significant thermal degradation of the MLI system due to purging, pumpdown, or repressurization, and thermal cycling was noted. A significant difference in the MLI temperature history during the transition from ground-hold to space-hold conditions due to the presence of water vapor within the MLI system was noted. After the MLI had been subjected to moisture, the space-hold heat input increased to as much as 8.91 watts (30.4 Btu/hr, a 19-percent increase over the nominal thermal performance. Increasing the gaseous-helium purge temperature from 300 to 344 K (540° to 620° R) was not effective in completely removing the moisture from within the MLI panels. The final measured space-hold thermal performance, after attempting to remove the moisture by vacuum pumping, was 8.04 watts (27.5 Btu/hr). Posttest inspections revealed no structural damage to the insulation and no degradation of the emissivity of the radiation shields.

INTRODUCTION

Within the last several years, the concept of a reusable cryogenic upper stage vehicle to be used to deliver and/or retrieve spacecraft from geosynchronous orbit has been proposed as a part of the Space Shuttle transportation system. Such an upper stage vehicle requires multilayer insulation (MLI) to provide the necessary space-hold (vacuum) thermal protection for the cryogenic propellants carried on the vehicle, particularly for near-Earth orbital operations of a few days or longer. To be cost effective, the MLI on the propellant tanks must itself be reusable (e.g., ref. 1). This requires that the heat input through the MLI must be predictable and must remain relatively constant from one space flight to the next during the required life expectancy of the insulation system. To enable the MLI to provide reliable thermal performance, the insulation system must be designed to meet all the environmental conditions imposed by such a series of space flights. These environmental conditions include (1) purging the MLI to remove condensible gases both prior to and during the filling of the propellant tank with a cryogen, (2) 1-atmosphere pressure ground-hold conditions (including continued purging of the MLI), (3) venting the MLI during atmospheric ascent, (4) vacuum space-hold conditions, and (5) purging and repressurizing the MLI during the atmospheric reentry with the vehicle in the cargo bay of the Space Shuttle Orbiter.

The analytical and experimental test results of one potentially reusable MLI system were reported in reference 2. This MLI system used double-goldized Kapton (DGK) radiation shields separated by Dacron tufts. The MLI system was enclosed in a purge bag surrounding the propellant tank. Purging and repressurizing the MLI system was accomplished by flowing gaseous helium through purge pins penetrating the MLI and then directly between the individual radiation shields. The MLI system was subjected to 100 thermal-environmental cycles representative of typical cryogenic spacecraft flight conditions. Space-hold thermal performance data for the MLI system were obtained periodically during the test program. The total measured heat input was observed to degrade up to 23 percent during the test program with most of the degradation attributed to the separation of three seams between adjacent MLI gore panels caused by the structural failure of several plastic links joining the panels.

A second potentially reusable MLI system (ref. 3) was also designed, fabricated, and tested for space-hold thermal performance. This MLI system used double-aluminized Mylar (DAM) radiation shields separated by double silk net spacers. A purge bag was not incorporated as a part of the design of this MLI system. The proposed purge technique relied on introducing the helium purge gas under the MLI blankets as well as into the volume surrounding the insulated tank. The purge gas would then be expected to diffuse into the insulation panels between individual radiation shields to displace the condensible gas therein initially. However, no experimental evaluation of the proposed

purge technique was conducted, and only space-hold thermal performance test results for this particular MLI system were reported in reference 3.

It was of interest, therefore, to conduct additional experimental tests with a DAM/silk net MLI system to further explore its potential for being classified as a reusable insulation system. This type of insulation system, compared to the DGK/Dacron tuft MLI system reported in reference 2, could potentially provide the following advantages: (1) lower cost, (2) ability to fabricate MLI panels conforming to a double-curved tank contour while maintaining good control of the layer density, (3) greater ease of replacement of damaged MLI panels, and (4) lower weight due to the elimination of the fiberglass girth fairing and purge bag. In regard to the last point, it was assumed that the structural shell of the space vehicle (including propulsion vehicles as well as resupply vehicles carrying cryogenic fluids) could also act as the "purge bag."

In order to conduct the desired additional experimental tests, a 1.39-meter-(4.57-ft-) diameter spherical cryogenic propellant tank was insulated with a DAM/silk net MLI system in a manner very similar to that described in reference 3. The experimental test program was conducted in two parts: Part 1 (reported in ref. 4) was conducted to determine the purge characteristics of the MLI system; Part 2, reported herein, documents the results of experimental tests in which the insulation system was subjected to 19 thermal (environmental) cycles simulating the space vehicle flight conditions noted previously.

During each of these 19 thermal (environmental) cycles, the MLI system was subjected to a gaseous-helium purge at either 300 or 344 K (540° or 620° R) to displace the gaseous nitrogen and/or water vapor initially contained in the MLI system. Purging the MLI system was generally conducted for 3 hours. The measured purge gas concentrations within the MLI system at the end of the purge period were greater than 99 percent helium (less than 1 percent condensible gas remaining). One-atmosphere pressure ground-hold and vacuum space-hold thermal performance measurements were obtained for each thermal cycle with the propellant tank containing liquid hydrogen. Water vapor was added to the gaseous nitrogen (or, for two tests, helium) initially in the vacuum chamber and MLI system for the last seven thermal cycles to determine (1) the ability to purge moisture from within the MLI system and (2) the subsequent degradation of the MLI space-hold thermal performance.

Although test measurements were made primarily in the U.S. Customary Units system, the International System (SI) of Units is the primary system of units used in this report.

SYMBOLS

A	area, m^2 (ft^2)
C_d	discharge coefficient
$C_{1, 2, 3, 4}$	constants
D_{AB}	diffusion coefficient, m^2/min (ft^2/min)
d	differential
d_o	orifice diameter, cm^2 ($in.^2$)
h	enthalpy, W-hr/kg (Btu/lb)
IP	MLI interstitial pressure, N/m^2 (torr)
K	thermal conductivity, W/m-K (Btu/hr-ft-^oR)
LD	layer density, layers/cm (layers/in.)
ℓ	length, m (ft)
$\dot{m}$	purge gas mass flow rate, kg/hr (lbm/hr)
N	number of effective radiation shields
n	number of MLI gore panels per blanket
P	pressure, N/m^2 ($lb/in.^2$)
Q	heat input, W (Btu/hr)
q	seam heat input, W/m (Btu/hr-ft)
$\dot{q}$	heat flux, W/m^2 (Btu/hr-ft^2)
R	gas constant, J/kg-K (ft-lbf/lbm-^oR)
r	radius, m (ft)
T	temperature, K (^oR)
V	volume, m^3 (ft^3)
$\dot{v}$	purge gas volumetric flow rate, m^3/hr (ft^3/hr)
$\dot{w}$	measured liquid hydrogen boiloff mass flow rate, kg/hr (lbm/hr)
x	height MLI gore panel extends on conical section, m (ft)
ϵ	emissivity
θ	half-angle, deg
λ	latent heat of vaporization, W-hr/kg (Btu/lbm)

ρ density, kg/m^3 (lbm/ft^3)

$\overline{\rho}$ reflectance

Subscripts:

a apex of truncated cone

c cold

co conical MLI panel

cond conduction

g MLI gore panel

h hot

$\overline{h}$ hemispherical

L liquid

MLI multilayer insulation

$\overline{n}$ near normal

SV saturated vapor

s seam

TV tank vent

tot total

EXPERIMENTAL APPARATUS

The experimental test apparatus was designed to use the measurement of the liquid hydrogen boiloff flow rate as an indication of the total heat input into the test tank. This technique of colorimetry required taking several precautions to accurately determine the relatively low heat input into the test tank attributed to the multilayer insulation during the space-hold (vacuum) tests. These precautions included the following:

(1) Thermally shorting the plumbing lines and instrumentation wires associated with the test tank to a cold guard filled with liquid hydrogen to minimize the extraneous heat leaks into the test tank

(2) Maintaining the pressure and temperature of the liquid hydrogen in the cold guard slightly higher than that in the test tank to prevent condensation of the boiloff gas flow from the test tank

(3) Maintaining the test tank pressure at very nearly a constant value to reduce variations in the boiloff gas flow rate due to the heat storage capacity of the liquid hydrogen

(4) Measuring the boiloff gas temperature just prior to being vented from the test tank to account for heating the boiloff gas to some higher outlet temperature

(5) Maintaining a constant temperature environment (or shroud) surrounding the insulated test tank so that the measured heat inputs were directly comparable from one test to the next

Test Tank

The liquid hydrogen test tank (fig. 1) used in this test program was a spherical tank 1.39 meters (4.57 ft) in diameter that had a volume of 1.42 cubic meters (50 ft^3). The tank was constructed of 2219-T62 aluminum. The upper and lower hemispherical shells of the tank were chemically milled to a membrane thickness of 0.094±0.013 centimeter (0.037±0.005 in.); the weld lands were 0.41 centimeter (0.16 in.) thick. The test tank had a working pressure of 3.4×10^5 newtons per square meter differential (50 psid). The tank was supported by three support brackets welded to the lower hemispherical shell.

The test tank incorporated a 0.3-meter- (1-ft-) diameter access opening and cover to allow access to the tank interior. The access cover had four ports to accommodate a vent line, a dip-tube fill and drain line, an instrumentation rake, and an electrical feedthrough. A conical deflector was mounted on the access cover just under the entrance to the vent line inside the test tank. The purpose of this deflector was to minimize the entrainment of liquid hydrogen droplets in the boiloff gas flow venting from the tank during the high-heat-flux, ground-hold boiloff conditions. An instrumentation rake containing six platinum resistance thermometers (PRT's) to measure liquid hydrogen and ullage gas temperatures was also mounted on the access cover inside the test tank.

Multilayer Insulation System (MLI)

The MLI system installed on the liquid hydrogen test tank employed the same basic modular design as the MLI system previously tested for space-hold (vacuum) thermal performance and reported in reference 3. The basic insulation design concept used two MLI blankets (fig. 2) to cover and thermally protect the entire tank surface. Each blanket consisted of 15 DAM radiation shields alternately spaced with 16 double silk net spacers. A laminated, aluminized Mylar/Dacron scrim (reinforced Mylar) cover sheet was applied to each side of each blanket. The layup of cover sheets, radiation shields, and silk net spacers for each MLI blanket was held together by Nylon button-pin studs spaced on approximately 20-centimeter (8-in.) centers.

The portion of the MLI blankets installed on the sides of the test tank were fabricated in the shape of gore panels with each blanket of MLI containing six 60° gore panels

(fig. 3(a)). The panels were fabricated to conform to the nominal double-curved contour of the tank wall by using the following techniques:

(1) Forming the silk net spacers to the desired contour by wetting, stretching, and drying the silk netting on a male mold

(2) Partially forming the radiation shields by means of vacuum forming in a female mold and then completing the forming to the desired contour by cutting, folding, and taping the aluminized Mylar on a male mold

(3) Partially forming the cover sheets by vacuum forming in a female mold and then completing the forming to the desired contour by hand ironing the sheets over a male mold

The room temperature emissivity of several of the radiation shields was measured after forming the shields to the desired tank contour. The room temperature emissivity $\epsilon_{\text{tot},\bar{h}}$ of the radiation shields was the average value of total hemispherical emittance as determined by a Gier Dunkle reflectometer (model DB 100). The reflectometer provided a measurement of the near-normal reflectance $\rho_{\bar{n}}$ of the surface of a sample. The total hemispherical emittance $\epsilon_{\text{tot},\bar{h}}$ of the radiation shields was then calculated from the following equation as suggested by reference 5:

$$\epsilon_{\text{tot},\bar{h}} = 1.33\,\epsilon_{\bar{n}} = 1.33\left(1 - \rho_{\bar{n}}\right) \tag{1}$$

The total hemispherical emittance, as determined by averaging a total of 125 measurements on five different radiation shields, was 0.050.

MLI panels in the shape of truncated cones were used to thermally protect the top and bottom of the test tank. These panels were fabricated in a manner very similar to the 60° gore panels with the exception that partial vacuum forming the radiation shields and cover sheets was not required. Both the radiation shields and cover sheets were formed to the desired conical countour by simply cutting, folding, and taping flat sheets of the material over a male mold.

During the assembly of the MLI panels, the Nylon button-pin studs were cemented to the exterior surface of the cover sheets at their points of contact to further provide a positive means of layer density control. The nominal insulation panel layer density was approximately 18 layers per centimeter (45 layers per inch). This value was based on the Nylon button-pin stud length of 0.95 centimeter (0.38 in.); the effective thickness of each of the cover sheets of approximately 0.025 centimeter (0.010 in.) was also accounted for.

Also added to the MLI 60° gore panels during assembly were the items necessary to provide installation for the panels on the test tank. These items included strips of

Velcro hook and pile fastener and Nylon grommets. The location of the polyester Velcro fastener on the MLI gore panels is shown in figure 3. Short intermittent strips of Velcro pile 5.1 centimeters (2.0 in.) wide were adhesively bonded to the outer cover sheets adjacent to one edge of the panels for both the inner and outer blankets of insulation. Long continuous strips of Velcro hook 2.5 centimeters (1.0 in.) wide were adhesively bonded to the inward (toward the tank wall) facing portions of both the inner and outer cover sheets which extended beyond the edge of the MLI panels along each side as noted in figure 3(b).

Six Nylon grommets were also installed in each MLI gore panel (two near the top, two at the equator, and two near the bottom) as indicated in figure 4. The grommets completely penetrated the insulation panels and were retained in place by means of snap-on washers.

During assembly of the conical MLI panels for the top and bottom of the test tank, short strips of 2.5-centimeter- (1.0-in.-) wide Velcro fastener were adhesively bonded to the inner and outer cover sheets of the inner panels and the inner cover sheet of the outer panels. The general location of the Velcro fastener for the MLI panels at the bottom of the test tank (for example) is shown in figure 5. No Nylon grommets were installed in these conical MLI panels.

Installation of MLI Panels on Test Tank

Prior to installing the MLI panels, the following items (shown in fig. 6) were installed on the test tank: (1) vent and fill line tube connections, (2) two MLI gore panel purge rings, (3) two fiberglass cones, (4) two fiberglass cone purge tubes, (5) Velcro pile fastener, and (6) 36 Nylon positioning pins. The two circumferential purge rings were fabricated from 0.64-centimeter- (0.25-in.-) diameter aluminum tubing. Each purge ring contained 24 pairs of holes 0.033 centimeter (0.013 in.) in diameter equally spaced around the circumference of the tank. The holes in each pair were located on opposite sides (top and bottom) of the purge ring to more evenly distribute the helium purge gas underneath the MLI gore panels. The upper and lower fiberglass cones were used to support the conical MLI panels at the top and bottom of the tank. These cones were perforated with 0.32-centimeter- (0.125-in.-) diameter holes spaced on 2.0-centimeter (0.80-in.) centers to allow passage of the helium purge gas. The two 0.64-centimeter- (0.25-in.-) diameter cone purge tubes distributed helium purge gas under the fiberglass cones and conical MLI panels at the top and bottom of the tank. The short, intermittent strips of 5.1-centimeter- (2.0-in.-) wide Velcro pile fastener adhesively bonded to the tank wall were one means of attaching the MLI gore panels to the sides of the test tank. The 36 Nylon positioning pins were used to properly locate

the MLI gore panels on the test tank. The positioning pins also acted as a second means of attaching the gore panels to the tank. The base of each Nylon pin was adhesively bonded to the tank wall with a fiberglass cloth overlay and a thermoplastic polyester resin adhesive (Pliobond 4001/4004). The detail of the Nylon positioning pins, as well as the Nylon grommets mentioned previously, is noted in references 3 and 4.

The normal tank fill and drain elbow at the bottom of the tank (fig. 6) was blanked off and not used for this test program. Not shown in figure 6 are the strips of Velcro pile fastener adhesively bonded to the fiberglass cones to mate with the Velcro hook fastener on the inner cover sheets of the inner blanket conical MLI panels required for support of these panels.

The completed installation of the MLI system on the test tank is shown in figure 7. The installation of this system was also very similar to that described in reference 3. The inner blanket gore panels were installed as fabricated. The outer blanket gore panels, prior to installation, were cut back on the top and bottom (as shown in figs. 7 and 8) to mate with the outer blanket conical MLI panels in a standard butt joint. The inner cover sheets of the outer blanket gore panels, however, were left full length to fit over the Nylon positioning pins located near the top and bottom of the tank. The vertical butt joints between the MLI gore panels for the inner and outer blankets of insulation were offset 6^{o} as shown in figure 9 so that there would not be a direct path for thermal radiation to reach the tank wall. The overlapping cover sheets at each butt joint also provided additional protection from thermal radiation. Cutouts were made in all MLI gore panels to accommodate the penetration of the tank support brackets as shown in figure 10.

The conical MLI panels for the inner blanket of insulation were then installed on the top and bottom of the tank. The edges of these conical MLI panels were attached intermittently to the inner cover sheet of the MLI gore panels in the outer blanket with Velcro fasteners in a Y-type joint as shown in figure 8. The conical MLI panels in the outer blanket were then installed and mated with the MLI gore panels in the outer blanket with a standard butt joint with overlapping cover sheets.

Small, five-layer MLI panels (positioning pin covers) were installed over the protruding Nylon positioning pins and tank support brackets near the tank equator (figs. 7, 9, and 11) to prevent thermal radiation from reaching the tank directly. The positioning pin covers consisted of five radiation shields and six double silk net spacers with a reinforced Mylar cover sheet on each side. The positioning pin covers were held together with Dacron thread stitched around the outside edges. The covers were attached to the MLI gore panels of the outer blanket by means of Velcro fasteners and aluminized Mylar tape.

After the insulation system was installed on the test tank, the emissivity of several radiation shields at locations near the edge of the MLI gore panels was again measured

with a Gier Dunkle reflectometer. Despite the fact that nearly five years had passed since the original date of manufacture of the MLI gore panels, the average total hemispherical emissivity $\epsilon_{\text{tot, h}}$ of the 12 locations measured was 0.040. This value was somewhat less than the value of 0.050 noted previously because the earlier value included measurements near the center of the radiation shields where the emissivity had been degraded slightly due to the partial vacuum forming of the shields.

The weights of the various components of the MLI system are noted in table I. The weight of the ideal MLI panel of 0.511 kilogram per square meter (0.105 lb/ft^2) is for a flat panel made without resorting to vacuum forming or any cutting, folding, and taping of the radiation shields. The weights of the MLI system panels installed on the test tank were calculated by using these component weights. These calculated weights are compared in table II with the actual weights of the MLI system panels determined once the test program had been completed. Overall, the MLI system weight (excluding the fiberglass cones) was approximately 10 percent greater than that calculated. Most of this difference is probably due to the fact that the calculated MLI panel weights do not account for overlapping, folding, or taping the individual radiation shields or for such items as aluminized Mylar tape, adhesive, or thread used in fabricating the MLI panels.

Installation of Test Tank in Vacuum Chamber

All tests were conducted with the insulated test tank mounted within a cylindrical vacuum chamber 1.83 meters (6.00 ft) in diameter by 3.12 meters (10.25 ft) high. Three 0.25-meter (10-in.) oil diffusion pumps provided a vacuum capability in the low 10^{-3} newton per square meter (10^{-5} torr) range at ambient temperature conditions and in the low 10^{-4} newton per square meter (10^{-6} torr) range with the test tank filled with liquid hydrogen.

The insulated test tank was suspended from a tubular, stainless-steel support ring by six stainless-steel wire support struts 0.24 centimeter (0.094 in.) in diameter and 24.0 centimeters (9.46 in.) long (fig. 10). The tubular support ring was, in turn, suspended from the lid of the vacuum chamber by six support rods (fig. 12). The insulated test tank was enclosed in an electrically heated cylindrical shroud. The temperature of the shroud could be maintained within ±1.1 K (2.0° R) of a desired temperature during the helium purge tests and the space-hold thermal performance tests. The shroud consisted of five curved aluminum panels on the sides and two flat aluminum panels on the top and bottom. The vertical joints between adjacent side panels and the horizontal joints between the semicircular top and bottom panels were (1) open to allow purge gases to flow in and out of the shroud and (2) optically dense (see fig. 12) so that no direct thermal radiation from the vacuum chamber wall could reach the outer surface of

the insulation system. The shroud was bolted to the tank support ring for support.

A liquid hydrogen cold guard (0.76 m (2.5 ft) in diameter and 0.51 m (1.67 ft) high) was located above the test tank as shown in figure 12. This cold guard was to minimize any extraneous heat leaks to the test tank during the space-hold thermal performance tests. All purge tubing and instrumentation wiring that led to instrumentation located on or within the test tank was thermally shorted directly to the wall of the cold guard. The four purge tubes leading to the test tank were brazed to the wall of the cold guard (fig. 13(a)). The instrumentation wiring was adhesively bonded with the thermoplastic polyester resin adhesive mentioned earlier and clamped to the wall of the cold guard (fig. 13(b)). The test tank vent and fill lines passed directly through the cold guard and incorporated nearly right-angle bends to minimize extraneous heat leaks (including radiation tunneling) from this source. The cold guard was insulated with two blankets of MLI in very much the same manner as the test tank. The cold guard contained a sufficient volume of liquid hydrogen such that it did not require refilling during a $4\frac{1}{2}$-day space-hold thermal performance test. A photograph of the insulated test tank and cold guard is shown in figure 14.

Lead wires for the temperature sensors (thermocouples) located within the MLI system were thermally conditioned by running the lead wires along the reinforced Mylar cover sheets to which the sensors were attached all the way to the top of the test tank. The lead wires were then run up the vent line and to the top of the cold guard before they were brought out from within the insulation system. Lead wires to temperature sensors located on the outside surface of the MLI system were not thermally conditioned since the outer surface temperature of the insulation was very close to the ambient shroud temperature during the purge and space-hold thermal performance tests.

Purge Gas System

The purposes of the purge gas system were to allow (1) purging the MLI on both the test tank and cold guard with gaseous helium, (2) purging the vacuum chamber with either gaseous helium or gaseous nitrogen, and (3) repressurizing both the MLI and vacuum chamber from vacuum conditions to a 1-atmosphere pressure with either gaseous helium or gaseous nitrogen. Helium purge gas was distributed to the two purge tubes and two purge rings located under the MLI on the test tank from a common MLI purge manifold. Four flow-control orifices downstream of the manifold were used to distribute the purge gas in the volumetric flow rates desired to each purge tube and purge ring. The range of flow-control orifice diameters was such that the purge gas volumetric flow rates to the four arbitrarily defined purge regions in the MLI system (shown in fig. 15) were relatively uniform on the basis of MLI system volumes per unit time. The calculated volume of each purge region was the volume between the outer

surface of the insulation and the wall of the test tank. The volumetric flow through each choked-flow flow-control orifice can be compared by looking at the relative values of the orifice diameters, which ranged from 0.0292 to 0.0318 centimeter (0.0115 to 0.0125 in.), and discharge coefficients, which ranged from 0.802 to 0.898.

The purge gas heater with a 300-watt (1020 Btu/hr) electric heating capability was installed between the cold guard and the test tank as shown in figure 13(a). This heater heated the helium purge gas for the MLI system on the test tank to 350 K (630° R) for those purge tests where this was desired.

Additional details of the purge gas system are given in reference 4.

MLI Gas Sampling System

The purpose of the MLI gas sampling system was to provide a means of determining the purge gas concentration within the MLI system during the purge tests. Twelve gas sampling tubes were provided to withdraw samples of purge gas from within the MLI system. Six tubes were used to obtain gas samples at the butt joints between adjacent MLI panels to determine the time-dependent boundary conditions at the edges of the panels. The other six tubes were used to obtain samples of purge gas from within MLI panels between the radiation shields. The specific gas sampling locations are shown in figure 16.

The gas sampling tubes were inserted laterally into the MLI system through the butt joints. The six tubes used to obtain gas samples from within the MLI panels themselves were located between the two silk nets between the two outer radiation shields in each panel to minimize any degradation to the thermal performance of the insulation system. All of the gas sampling tubes were fabricated from 0.102-centimeter (0.040-in.) outside diameter by 0.015-centimeter (0.006-in.) wall thickness stainless-steel tubing to minimize any disturbance to the MLI panels as well as any extraneous heat leaks from the tubes themselves.

The gaseous-nitrogen concentration of the gas samples from the individual gas sampling tubes was sensed by two commercial thermal conductivity cells, one for the gas samples obtained at the butt joints and one for the gas samples obtained from within the MLI panels. The gas sampling tubes were paired together for purposes of obtaining experimental data such that the gas sample obtained from within a given MLI panel was analyzed for gas concentration by one thermal conductivity cell at the same time as the gas sample obtained from the adjacent butt joint was analyzed by the second thermal conductivity cell.

Additional details of the MLI gas sampling system are given in reference 4.

Instrumentation

Temperatures of the MLI blankets as well as of the constant-temperature shroud, the warm ends of the tank support struts, the Nylon positioning pins, and the purge gases were measured with chromel-constantan thermocouples. The temperature profiles across the MLI system were measured at six locations: (1) one each on the upper and lower conical MLI panels, (2) one each on the lower half and at the equator of the MLI gore panels, and (3) two on the upper half of the MLI gore panels. At each location temperatures were measured for the inner and outer cover sheets of the inner and outer blankets of insulation. Two additional thermocouples were used to measure the temperature on the inside surfaces (cover sheets) of two of the positioning pin covers, one larger rectangular positioning pin cover and one smaller circular positioning pin cover. These thermocouples were fabricated from 0.020-centimeter- (0.008-in.-) diameter wire. The thermocouple junctions were adhesively bonded to the reinforced Mylar cover sheets of the MLI panels with double-stick Mylar tape for approximately 2.5 centimeters (1.0 in.). The thermocouple junctions and approximately 15 centimeters (6 in.) of the lead wires were then covered and taped to the cover sheet with aluminized Mylar tape. The thermocouple leads from the thermocouples located on the inner MLI blanket and the inner cover sheet of the outer blanket were further thermally conditioned by running the wires along the cover sheets to which the junctions were attached to the top of the test tank, along the vent line insulation, and around the cold guard up to the top. The leads were then withdrawn from the cold guard insulation and routed to electrical feedthroughs in the lid of the vacuum chamber. The reference junctions for all the chromel-constantan thermocouples were immersed in a liquid-nitrogen bath. The temperature measurements provided by these thermocouples had a probable error of ±4.0 K (±7.2° R) at liquid hydrogen temperature. This error was a minimum of ±0.83 K (±1.5° R) at approximately 140 K (252° R) and then increased to ±2.3 K (±4.2° R) at room temperature. Calculations of the probable error considered errors from such sources as sensor errors (e.g., span between measured and reference temperatures, inhomogeneity of wire, and variations in reference bath temperature) and digitizer errors (e.g., readout accuracy, resolution, and noise).

Additional temperature measurements were obtained in areas expected to be at or near liquid-hydrogen temperature using platinum resistance thermometers (PRT's) to improve the accuracy of these measurements. Six PRT's were mounted on an instrumentation rake within the test tank to measure liquid-hydrogen and ullage gas temperatures. These PRT's were located at ullage levels of 1.50, 5.19, 6.50, 7.95, 9.51, and 15.0 percent. Six PRT's were also located on the exterior surface of the test tank to measure tank wall temperatures. These PRT's were located on the access cover, on the access cover support ring, and on the tank wall itself at ullage levels of 2.0,

5.0, 10.0, and 20.0 percent. PRT's were also located on the cold ends of the tank support struts and on the tank vent and fill lines between the tank and cold guard. These PRT's as well as those on the exterior surface of the tank were adhesively bonded in place using a thermoplastic polyester resin adhesive (Pliobond 4001/4004). The copper lead wires for all these PRT's were thermally conditioned by adhesively bonding them to the wall of the cold guard (fig. 13(b)) before the leads were routed to the electrical feedthroughs in the lid of the vacuum chamber. Two additional PRT probes were mounted in the cold guard to monitor the liquid-hydrogen level in the guard. All of these temperature measurements had a probable error from ±0.07 to ±1.26 K (±0.12° to 2.27° R) at liquid-hydrogen temperature depending on the temperature range of the electrical bridge circuit employed. These ranges varied from 20 to 26.7 K (36° to 48° R) to 20 to 111 K (36° to 200° R). Calculations of the probable error considered errors from such sources as sensor errors (e.g., calibration and repeatability specifications), lead wire and electrical connector errors (thermal EMF), and bridge unit errors (e.g., accuracy and nonlinearity) as well as the digitizer errors noted previously.

The liquid-hydrogen boiloff flow rate under the relatively high-heat-flux ground-hold conditions was measured using two-different devices. A venturi with a throat diameter of 1.765 centimeters (0.695 in.) was used for the first seven ground-hold tests. Because the measured ground-hold boiloff rate was less than originally predicted, a flat plate orifice with a diameter of 1.524 centimeters (0.600 in.) was substituted for the venturi to improve the accuracy of the measurements for the remainder of the tests. Both flowmeters were calibrated prior to use. The venturi was designed to have a 1.4×10^4 newtons per square meter differential pressure (2.0 psid) at the predicted flow rate while the flat-plate orifice provided a pressure differential of approximately 1.0×10^4 newtons per square meter (1.5 psid) at the actual flow rates obtained.

The liquid-hydrogen boiloff flow rate under the relatively low-heat-flux space-hold conditions was measured using a mass flowmeter having a 0 to 3.4 standard cubic meter per hour (0 to 2 standard ft^3/min) range. The uncertainty associated with this meter was ±0.5 percent of full scale.

Two thermal conductivity cells were used to determine the gaseous-nitrogen concentration within the MLI system during the purge tests. The drift of the zero and full-scale outputs of the cells noted during the steady-state calibrations and transient data taking was minimized by zeroing and spanning the output of the cells frequently. In general, the error due to drift occurring during the purge tests was less than 3-percent-gaseous-nitrogen concentration when measuring nitrogen concentrations near 100 percent, and it was less than approximately 0.3-percent-nitrogen concentration when measuring nitrogen concentrations near 0 percent. The dynamic error was small compared to the anticipated error due to drift, and no corrections for instrument error due to dynamic response were applied to the experimental data. A time interval of approximately

eight time constants was allowed from the time the output of the thermal conductivity cells started to respond to a change in gaseous-nitrogen concentration when shifting from one gas sampling tube to the next until the time the final output reading was taken.

Test tank, cold guard, and vacuum chamber pressures, as well as purge gas pressures upstream of the flow-control orifices and ground-hold boiloff gas pressures at the flowmeters, were measured with bonded strain-gage transducers, which had an estimated uncertainty of ±0.25 percent of full scale. Vacuum levels within the vacuum chamber were also measured by thermocouple gages and ionization gages. The ionization gages were located on the wall of the vacuum chamber as well as within the constant temperature shroud.

Control Systems

The temperature of the constant-temperature shroud enclosing the insulated test tank was controlled in a closed-loop mode by four separate alternating current electrical heating circuits having a total capacity of approximately 10 000 watts (34 000 Btu/hr). The shroud was divided into four heating zones - top, bottom, and upper and lower halves of the cylindrical walls. The top and bottom zones each used two silicon rubber heating blankets wired in parallel. The upper and lower zones of the cylindrical walls each had five heating blankets wired in parallel (one blanket on each of the five side panels). Temperature control of the shroud during the space-hold thermal performance tests was maintained at 300±1 K ($540^{\circ}\pm2^{\circ}$ R).

Temperature control of the purge gas heater was also provided in a closed-loop mode by a 300-watt (1020-Btu/hr) silicon rubber heater and controller.

Repressurization of the MLI system and vacuum chamber from vacuum conditions to a 1-atmosphere absolute pressure was accomplished by opening two flow-control valves in the purge gas system on a preselected schedule. The valves were opened such that (1) purge gas flow rates into the MLI system and vacuum chamber would be controlled in an attempt to provide a slight positive pressure within the MLI system and (2) the pressure rise rate in the vacuum chamber would approximate that expected in the cargo bay of the Space Shuttle Orbiter (ref. 7).

The test tank and cold guard pressures were maintained at a constant level during the space-hold thermal performance tests by two separate closed-loop control systems as shown in figure 17. These pressure-control systems used high resolution, differential-pressure, capacitance transducers which sensed very small pressure variations inside the test tank and cold guard relative to an absolute reference pressure. The electrical output signals from the transducers were used as input signals to control units for the motorized pressure-regulating valves in the test tank and cold guard vent

lines. Opening and closing the motorized valves regulated the liquid-hydrogen boiloff flow rates to maintain the tank pressures at constant values. The reference pressure was provided by a 0.0148-cubic-meter (0.523-ft^3) gaseous-nitrogen tank maintained at a constant temperature by an ice bath. This system maintained the test tank and cold guard pressures to within 5.5 newtons per square meter (0.0008 psi) of the reference tank pressure. This reduced the potential variations in the boiloff gas flow rate due to the heat storage capacity of the liquid hydrogen so that errors in the total measured heat input caused by fluctuations in tank pressure were less than approximately 0.5 percent of the measured value. The reference pressure varied from test to test depending on the test tank pressure variations experienced when the tank was filled and subsequently topped-off with liquid hydrogen. The reference tank pressure was always set lower than the minimum test tank pressure experienced while loading liquid hydrogen; the pressures used varied from 1.07×10^5 to 1.21×10^5 newtons per square meter (15.5 to 17.5 psia). In addition, the cold guard pressure was maintained between 70 and 210 newtons per square meter (0.01 to 0.03 psia) above that of the test tank so that no condensation of the boiloff gas from the test tank would occur as the boiloff gas flowed through the portion of the vent line passing through the cold guard.

Data Recording

Most of the experimental data were recorded by a high-speed digital data system. Additionally, some of the data such as the test tank, cold guard and vacuum chamber pressures, liquid-hydrogen boiloff rate, shroud temperatures, output of the capacitance-type differential pressure transducers in the tank pressure control system, and the output of the thermal conductivity cells in the gas sampling system were recorded on strip charts in the control room. A small amount of data was also recorded by hand from digital panel meters located in the control room.

TEST PROCEDURE

Purge Test

Prior to each gaseous helium purge test, the vacuum chamber was evacuated to a vacuum level of 10 newtons per square meter (0.08 torr) or less to purge the MLI system and vacuum chamber of any gases remaining from the previous test. The chamber was then slowly backfilled with clean, dry gaseous nitrogen to 1 atmosphere absolute pressure over a period of about 1 hour. For the series of tests concerned with the degradation of the MLI thermal performance due to the presence of moisture, the chamber

was initially blackfilled to slightly less than a 1-atmosphere absolute pressure. A sufficient quantity of distilled water was then added to the chamber, primarily through the chamber vent line, to create a 100-percent relative humidity environment within the chamber. The MLI system was exposed to this environment for periods ranging from 2 hours to 56 days before continuing with the test.

Gas samples were then generally taken from within the MLI system to check the gas sampling system operation and confirm the presence of 100-percent nitrogen gas. The purge system gas supply pressures were set to provide the desired purge gas flow rates, and the shroud heater and purge gas heater controllers were set at either 300 or 350 K (540° or 630° R) depending on the test requirements. The 350 K (630° R) shroud temperature was required to obtain the desired 344 K (620° R) temperature of the MLI system during the time allotted for the purge test. At the start of the purge test, the heaters were turned on and the MLI system and vacuum chamber helium purge flows were started simultaneously. The purge gases were vented near the bottom of the vacuum chamber. Gas samples from within the MLI system were withdrawn for 1 minute each through the 12 gas sampling tubes at fairly regular intervals during the purge test. These intervals were, approximately, either $\frac{1}{2}$ or 1 hour. The purge tests were continued for 3 to 4 hours to insure that the gaseous-nitrogen concentrations at all the gas sampling locations had been reduced to less than 1 percent.

Ground-Hold Thermal Performance Test

After the purge test had been completed, the purge gas heater was turned off, and the shroud heater controllers were set at 300 K (540° R). The gaseous helium purge flow rates for both the MLI system and the vacuum chamber were reduced to the desired values for the ground-hold tests. The test tank was then filled with liquid hydrogen over approximately $\frac{1}{2}$ hour. Once the tank was full, as indicated by the platinum resistance thermometers located inside the tank, a reduced flow of liquid hydrogen into the tank was maintained until the PRT located on the access cover indicated that the cover had chilled down to near the liquid-hydrogen temperature. During this fill procedure, the test tank pressure was maintained at approximately 1.4×10^5 newtons per square meter (20 psia). To measure the ground-hold liquid-hydrogen boiloff flow rate, the tank pressure was reduced and maintained at 1.24×10^5 newtons per square meter (18.0 psia). The 4-kilowatt (13 660-Btu/hr) heater in the facility vent line (fig. 17) was turned on to increase the boiloff gas temperature, and hence the volumetric flow, through the measurement device to improve the accuracy. Approximately 10 minutes were required for the tank pressure to stabilize, and another 10 to 20 minutes were required for the boiloff flow rate to reach a relatively constant value. The differential

pressure was then measured across either the venturi or the flat-plate orifice flow measurement device. The liquid-hydrogen fill level in the test tank was generally between the 5 and 6.5 percent ullage levels when the boiloff flow rate measurement was made.

Space-Hold Thermal Performance Test

After the ground-hold thermal performance test had been completed, the vacuum chamber was evacuated to vacuum conditions at a rate as fast as the test facility pumping capability would allow. The oil diffusion pumps were cut in at a vacuum level of approximately 10 newtons per square meter (8×10^{-2} torr), and a vacuum level of approximately 0.1 newton per square meter (8×10^{-4} torr) could be reached within 12 to 15 minutes after the start of the pumpdown. Times as long as 20 to 30 minutes were required to reach this vacuum level because of increased outgassing if the MLI system had been exposed to water vapor. The cold guard was then filled with liquid hydrogen, the test tank was retopped until full, and the access cover had again chilled down to the liquid-hydrogen temperature. The reference pressure in the tank pressure control system was set slightly lower than the minimum test tank pressure experienced during the filling and retopping procedure (1.07×10^5 to 1.21×10^5 N/m^2 (15.5 to 17.5 psia)), and the back pressure control system was brought online to control the pressures in the test tank and cold guard. The liquid-hydrogen boiloff gas was vented through the 0 to 3.4 standard cubic meter per hour (0 to 2 standard ft^3/min) mass flowmeter as soon as the flow rate was within that range. The test was continued until steady-state MLI system temperature and liquid-hydrogen boiloff flow rate conditions had been achieved; generally, about 3 days were required. Steady-state MLI system temperature conditions were assumed to have been achieved when the temperatures did not change more than 0.56 K (1.0° R) over a period of at least 5 hours.

For tests 1, 3, 5, 7, 9, and 18, where the tests were dedicated to measuring only the vacuum space-hold thermal performance of the insulation system, the initial test procedure was somewhat different. The vacuum chamber was evacuated to the 10^{-3} newton per square meter (10^{-5} torr) range with the insulation system at ambient temperature for approximately $2\frac{1}{2}$ days to reduce any outgassing occurring within the insulation to a relatively low value. The test tank and cold guard were then filled with liquid hydrogen at approximately 1.4×10^5 newtons per square meter (20 psia). Once the tanks had been filled, the back-pressure control system was brought online, and the test was completed in the same manner as noted previously.

Repressurization Test

After the space-hold thermal performance test had been completed, the remaining liquid hydrogen was removed from the test tank and cold guard. The flow lines in the purge gas system between the vacuum chamber isolation valves and the two flow-control valves mentioned earlier were vacuum purged. The gaseous-helium supply pressures upstream of the flow control were set to the desired values. The three oil diffusion pumps were then valved off, and the repressurization sequence was started. The flow-control valves were opened on a predetermined schedule (1) to provide a rate of increase of the pressure in the vacuum chamber to approximate that expected in the cargo bay of the Space Shuttle Orbiter during atmospheric reentry and (2) to maintain a positive pressure differential across the MLI system. When the chamber pressure reached a 1-atmosphere absolute pressure, the chamber vent valve was opened, and the test was terminated.

DATA REDUCTION

Purge Gas Flow Rates

The purge gas flow rates for the MLI system and the free volume of the vacuum chamber were calculated in terms of the mass flow rate and the volumetric flow rate. The volumetric flow rates, normalized in terms of the number of volumes per hours, were calculated from

$$\frac{\dot{V}}{V} = \frac{\dot{m}}{\frac{P}{RT} V} \tag{2}$$

where, for the MLI system,

T average MLI temperature, K (^{o}R)

V MLI system volume, m^3 (ft^3)

P vacuum chamber pressure, N/m^2 (psia)

or, for the free volume of the vacuum chamber,

T average shroud temperature, K (^{o}R)

V vacuum chamber free volume, m^3 (ft^3)

P vacuum chamber pressure, N/m^2 (psia)

The volume of the MLI system was calculated to be 0.186 cubic meter (6.58 ft^3) while the free volume of the vacuum chamber was calculated to be 5.695 cubic meters (201.1 ft^3).

Measured Heat Inputs

The total heat input into the test tank during both the ground-hold and space-hold thermal performance tests was calculated from

$$\dot{Q}_{tot} = \dot{w}\lambda\left(\frac{\rho_L}{\rho_L - \rho_{SV}}\right) + \dot{w}(h_{TV} - h_{SV}) \tag{3}$$

The density ratio factor is a correction for the portion of the liquid-hydrogen boiloff that was not vented from the test tank but merely occupied the space vacated by the evaporated liquid. The second term takes into account the heating of the remaining boiloff gas to some higher outlet temperature prior to being vented from the tank. The value of the enthalpy of the boiloff gas at the tant vent (h_{TV}) was evaluated at the ullage gas temperature indicated by the PRT located inside the tank at the 1.5-percent ullage level.

Extraneous heat inputs into the test tank attributed to the PRT instrumentation wires, purge tubing, vent and fill lines, tank support struts, and Nylon positioning pins were assumed to result from solid conduction heat transfer. The heat inputs were calculated from measured temperatures and thermophysical properties of the materials involved using the Fourier heat-transfer equation

$$Q_{cond} = \frac{A}{\ell}\int_{T_c}^{T_h} K(T)dT \tag{4}$$

Predicted Ground-Hold Thermal Performance

The heat input through the MLI system into the test tank during the ground-hold conditions was predicted assuming gaseous-helium conduction heat transfer through each blanket of insulation using the measured temperatures of the cover sheets for each test. The increased overall thickness of the insulation system in the areas near the top and bottom of the test tank where the inner conical MLI panels overlapped the inner MLI gore panels (fig. 12) was accounted for. Overall, the ground-hold heat flux was calcu-

lated to be approximately 690 watts per square meter (220 Btu/hr-ft^2) assuming the thickness of each MLI blanket was 0.95 centimeter (0.38 in.).

Predicted Space-Hold Thermal Performance

The predicted heat input into the test tank attributed to the basic thermal performance of the multilayer insulation was calculated using the following equation obtained from reference 5:

$$\dot{q}_{MLI} = \frac{C_1 (LD)^{2.56}}{N-1}\left(\frac{T_h^2 - T_c^2}{2}\right) + \frac{C_2 \epsilon_{tot,\bar{h}}}{N-1}\left(T_h^{4.67} - T_c^{4.67}\right) + \frac{C_3 (IP)}{N-1}\left(T_h^{C_4} - T_c^{C_4}\right) \qquad (5)$$

where

$$C_1 = 8.95\times10^{-8}$$

$$C_2 = 5.39\times10^{-10}$$

For a gaseous nitrogen background (test 1),

$$C_3 = 1.10\times10^{2}$$

$$C_4 = 0.52$$

and for a gaseous helium background (tests 7 and 18)

$$C_3 = 3.67\times10^{2})$$

$$C_4 = 0.26$$

The average measured temperatures of the inside and outside cover sheets of the MLI system were used for temperatures T_c and T_h, respectively. The outside surface areas of the conical MLI panels and MLI gore panels of 2.279 and 4.555 square meters (24.53 and 49.03 ft^2), respectively, were used to calculate the total predicted MLI heat input.

The predicted MLI temperature profiles were calculated by using the initially predicted MLI heat flux along with equation (5) to calculate the individual radiation shield

temperatures, starting with the inner cover sheet temperature and working toward the next warmer radiation shield.

The heat input into the test tank due to the presence of the seams or butt joints between adjacent MLI panels was estimated using a value for seam degradation of 0.169 watt per meter (0.176 Btu/hr-ft) of seam length determined in reference 6. This value was determined for an offset butt joint with overlapping cover sheets, which is the typical seam configuration for the butt joints between adjacent MLI gore panels (fig. 9). There were approximately 7.22 meters (23.7 ft) of seams (primarily between adjacent MLI gore panels) in this MLI configuration tested. The length of the butt joints between the inner blanket MLI gore panels extending past the outer blanket MLI gore panels near the top and bottom of the test tank were neglected. There were also approximately 6.37 meters (20.9 ft) of seams between the MLI gore panels and the conical MLI panels at the top and bottom of the test tank. Although this seam configuration (as shown in fig. 8) did not match exactly the standard offset butt joint configuration used between adjacent MLI gore panels, the same value for seam degradation noted previously was arbitrarily assumed for the thermal degradation.

The heat input into the test tank due to the thermal degradation of the multilayer insulation in the vicinity of the tank support struts was also estimated by using a value of 0.403 watt (1.376 Btu/hr) for each penetration as determined in reference 6. Any effect of the relatively close spacing between the tank support struts for each of the three pairs of struts was neglected.

RESULTS AND DISCUSSION

The results of the experimental test program are discussed under five main headings:

1. Space-Hold Thermal Performance - Results from tests 1, 3, 5, 7, 9, and 18, which were dedicated to measuring only the thermal performance of the insulation system under vacuum conditions
2. Ground-Hold Thermal Performance - Results from test 8, which was dedicated to measuring only the thermal performance of the insulation system with gaseous helium at a 1-atmosphere pressure within and surrounding the insulation
3. Thermal Cycles - Results from tests 10-1 to 13, in which the complete thermal cycle of gaseous-helium purging, liquid-hydrogen fill, ground-hold conditions, vacuum chamber pumpdown, transition to vacuum space-hold conditions, and repressurization of the insulation system and vacuum chamber back to a 1-atmosphere pressure were imposed

4. Degradation Due to Moisture - Results from tests 14 to 17, which had essentially the same test conditions as the thermal cycle tests except that the insulation system was subjected to a 100-percent relative humidity environment prior to starting each test
5. Posttest Inspection - Results of inspecting the MLI system after all testing was completed

The previous test history of the MLI system reported in reference 4 is summarized in table III. These tests were primarily ambient temperature helium purge tests. The tests were interspersed with four space-hold thermal performance tests to determine if anything done to the MLI system during the conduct of the purge tests had affected the thermal performance of the insulation system.

The basic test sequence of the test program reported herein is shown in table IV. The tests were numbered such that all tests in a given series (test 10, e.g.) had nearly identical test conditions; the -5, for example, indicated that this was the fifth such test in the series. Test 8 was conducted to determine the initial ground-hold thermal performance of the insulation system. This test was followed by another space-hold thermal performance test to again determine if the ground-hold conditions had done anything to alter the thermal performance of the insulation under vacuum conditions. The thermal cycles imposed on the insulation system by simulating the environmental conditions of a typical space mission were started with test 10-1. For tests 10-1 to 10-5, these environmental conditions included (1) purging the MLI to remove condensible gases prior to filling the propellant tank with liquid hydrogen, (2) 1-atmosphere pressure ground-hold conditions, (3) venting the MLI during atmospheric pressure decay to vacuum conditions, and (4) vacuum space-hold conditions. For the experimental tests starting with test 11-1, the environmental conditions simulating repressurization of the MLI system during atmospheric reentry were added to complete the thermal cycle. Water was added to the vacuum chamber for varying periods of time before starting the purging to provide an initial 100-percent relative humidity environment for tests 14-2 to 17-2. The final test (test 18) was another space-hold thermal performance test in which the MLI system was subjected to a vacuum environment (to outgas any residual water left within the insulation from previous tests) for 5 days prior to filling the test tank with liquid hydrogen.

Space-Hold Thermal Performance

The total measured heat input into the test tank for the space-hold thermal performance tests along with the measured component heat inputs through the tank support struts, the Nylon positioning pins, and other extraneous sources are shown in table V.

Subtracting the component heat inputs from the total tank heat input leaves the total heat input attributed to the multilayer insulation itself. The initial baseline space-hold heat input (test 1) attributed to the MLI was 7.18 watts (24.5 Btu/hr). The MLI heat input for the first four tests averaged 7.40 watts (25.3 Btu/hr) with a maximum deviation of 6 percent. This is a relatively small deviation in the experimental data considering the purge testing conducted between the thermal performance tests and the general nature of the heat transfer through multilayer insulations. This average heat-transfer rate corresponds to a boiloff rate of 1.45 percent of the tank volume per day.

The measured temperature profiles through the MLI for tests 1 and 7 are shown in figure 18. The only significant difference between the two temperature profiles is the lower temperatures of the inner cover sheet of the inner blanket MLI gore panels for test 7. This difference was apparently due to the fact that test 7 followed the initial 344 K (620° R) temperature purge test (test 6B), which may have caused the inner blanket gore panels to more fully conform to the shape of the tank wall and thus allow more intimate contact with the wall. The basic heat input through the MLI gore and conical panels was calculated using the measured hot and cold insulation boundary temperatures shown in figure 18 along with equation (5). The resulting calculated basic MLI heat inputs are shown in table V along with the MLI thermal degradation calculated for the seams and tank support strut penetrations. The total calculated MLI heat input was 7.94 and 8.00 watts (27.1 and 27.3 Btu/hr) for tests 1 and 7, respectively. These predicted heat inputs are of the order of 8 percent higher than the average measured heat input.

Also shown in figure 18 are the calculated MLI temperature profiles for tests 1 and 7. The profiles were calculated using equation (5) and moving from shield to shield starting with the coldest radiation shield (cover sheet). The calculated profiles compare reasonably well with the experimental data.

The space-hold thermal performance for test 9 that was obtained after the initial ground-hold thermal performance test indicated a slightly lower heat input to the test tank than measured previously (table V). The reason for this is not specifically known. However, imposing the ground-hold environmental conditions on the MLI system certainly did not degrade the subsequent space-hold thermal performance, which was the primary question to be resolved.

Ground-Hold Thermal Performance (Test 8)

Test 8 was the first experimental test in which the MLI system was subjected to a ground-hold environment. The MLI system and vacuum chamber contained 100-percent gaseous helium. The helium purge rates were 0.22 and 1.03 kilograms per hour (0.49 and 2.27 lb/hr) for the MLI system and the vacuum chamber, respectively. The MLI

system purge rate was chosen such that a positive flow of helium purge gas out of the MLI system would still be expected throughout the transient temperature conditions existing for a tank fill and insulation chilldown time of 20 minutes. The liquid-hydrogen boiloff rate measured with the venturi was 24.5 kilograms per hour (54.0 lb/hr), and the ullage gas temperature within the test tank at the vent line was 30.2 K (54.3° R), which resulted in a measured heat input of 3848 watts (13 140 Btu/hr). Of this value, approximately 3.0 watts (10 Btu/hr) were composed of extraneous heat inputs (as noted in the DATA REDUCTION section) so that the heat input attributed directly to the MLI system was 3845 watts (13 130 Btu/hr). This heat input corresponds to a boiloff rate of 31.4 percent of the tank volume per hour. The liquid-hydrogen level in the tank for this particular test was between the 9.5- and 15.0-percent ullage levels.

The predicted heat input for this ground-hold test was 4762 watts (16 260 Btu/hr). Therefore, the measured heat input was approximately 19 percent lower than the predicted heat input. This discrepancy between the measured and predicted values could not be accounted for since the predicted heat input was based on using five local insulation temperature profiles in different areas of the MLI system along with the thermal conductivity values for gaseous helium. One possible explanation is that the individual MLI blankets became "fluffed-up" slightly during the ground-hold purge conditions, thereby increasing the nominal thickness of the insulation.

An additional test was conducted during this overall ground-hold thermal test to try to determine the apparent density of the liquid hydrogen within the test tank under the relatively high heat-flux conditions. This information is desirable since it determines the maximum mass of liquid hydrogen that can be loaded into the tank when the liquid is boiling vigorously and has gas bubbles entrained within the bulk liquid. During this test, the PRT's within the test tank were used as liquid level sensors. The lower five PRT's on the instrumentation rake ranged from 20.0 to 26.7 K (36° to 48° R) and responded quickly (within a few seconds) to the increased ullage gas temperature when the sensors emerged from the liquid hydrogen. The test procedure was to (1) note when the normal-boiling liquid-hydrogen surface had just passed one PRT, (2) rapidly pressurize the test tank with ambient temperature gaseous hydrogen to suppress the boiling, and (3) note how manyPRT's emerged from the liquid as the liquid level decreased due to the momentary collapse of vapor bubbles within the liquid. The test results for two tests are noted in table VI. In the first of these tests, the initial liquid level started at the 5.19-percent ullage level. As the tank was pressurized, the next three lower PRT's emerged from the liquid, but the PRT located at the 15-percent ullage level did not. In the second test, the initial liquid level started at the 6.50-percent ullage level. After 38.4 seconds, the PRT located at the 15-percent ullage level indicated that it was uncovered. The liquid surface probably did not drop much past this level. In this case, the change in liquid volume between the boiling and nonboiling conditions was 0.121

cubic meter (4.26 ft^3). The calculated apparent density of the normal-boiling liquid hydrogen at a 1-atmosphere pressure would then be 64.4 kilograms per cubic meter (4.02 lb/ft^3). This represents a reduction of 9 percent from the normal density of nonboiling liquid hydrogen.

Thermal Cycles (Tests 10-1 to 13)

MLI temperature history. - Tests 10-1 to 13 were basically thermal cycling tests to determine if repetitive thermal cycling of the insulation system during simulated space-flight environmental conditions would degrade the thermal performance of the insulation. The test conditions were varied somewhat during these 11 tests as noted in table IV. The temperature history of the MLI during a typical test (e.g., test 11-3) is shown in figure 19. The temperatures shown are for thermocouples on the cover sheets of the two MLI blankets located on the lower half of the MLI gore panels. The temperatures noted as being for the intermediate cover sheets are the average temperatures for the outer sheet of the inner blanket and the inner cover sheet of the outer blanket of insulation. These temperatures were generally within a few degrees of each other. These temperature data were obtained in the control room from the digital panel meters. The MLI system was initially purged with gaseous helium for slightly more than 3 hours with the purge gas and shroud heaters set at 350 K (630° R) for this test. The insulation reached 344 K (620° R) for approximately the last hour of the purge test. The purge gas heater was then shut off, and the shroud heaters were reset to 300 K (540° R). The test tank was filled with liquid hydrogen, and the ground-hold conditions were established. During this time the insulation temperatures decreased rapidly to the normal ground-hold temperature profile, and the liquid-hydrogen boiloff flow rate was determined. The nominal ground-hold temperatures were approximately 215, 145, and 20 K (387°, 261°, and 36° R) for the outer, intermediate, and inner cover sheets, respectively. The vacuum chamber was then pumped down to vacuum conditions as rapidly as possible. During this time, the cold helium purge gas adjacent to the tank wall vented through the MLI system caused the outer and intermediate cover sheet temperatures to decrease rapidly to approximately 140 and 80 K (252° and 144° R), respectively. The outer cover sheet temperature recovered quickly and reached its final steady-state space-hold temperature of 299 K (539° R) within several hours. The intermediate cover sheet temperature increased more slowly and did not reach its final steady-state value of 227 K (409° R) until more than 60 hours after the vacuum chamber had been pumped down. The same was true of the inner cover sheet which finally reached a steady-state temperature of 35.6 K (64° R). After the final steady-state space-hold thermal performance measurements had been recorded, the test tank was

pressurized and the liquid hydrogen was drained from the tank. The variations in the insulation temperatures noted during this time were due to a partial loss of vacuum in the vacuum chamber caused by tubing connections experiencing transient temperatures and leaking slightly. After draining the test tank, vacuum levels in the chamber were restored to the $\sim 2 \times 10^{-2}$ newton per square meter (1×10^{-4} torr) range. The vacuum chamber and insulation system were then repressurized to a 1-atmosphere pressure with gaseous helium; this condition provided the resulting variations in the insulation temperature as shown in figure 19.

Vacuum chamber pressure history. - Typical vacuum chamber pressure histories for the pumpdown and repressurization phases of the tests are shown in figure 20 (again for test 11-3). During the pumpdown only the time period from 8 to 12 minutes provided a reasonable simulation of the rate of pressure decay to be expected in the cargo bay of the Space Shuttle Orbiter (ref. 7); the rate of pressure decay in the first 8 minutes was, in general, too slow. The vacuum chamber repressurization did provide a reasonably good simulation of the environment expected in the cargo bay of the Space Shuttle Orbiter.

Purge test results. - The results from the gaseous-helium purge phase of tests 10-1 to 13 are shown in figure 21. The gaseous-helium purge rates for these tests (shown in table IV) for the MLI system of approximately 0.95 and 1.10 kilograms per hour (2.1 and 2.4 lb/hr) and for MLI temperatures of 344 and 300 K (620° and 540° R), respectively, resulted in purge rates of approximately 36 MLI volumes per hour. Likewise, vacuum chamber purge rates of approximately 1.8 and 2.2 kilograms per hour (4.0 and 4.9 lb/hr) for shroud temperatures of 351 and 300 K (632° and 540° R), respectively, provided helium purge rates of approximately 2.4 vacuum chamber volumes per hour. These were approximately the same as the test conditions for tests 2D-1, 2D-2, 4A, 4B, and 6B for the test program previously conducted (table III).

The measured gaseous-nitrogen concentration as a function of time from the start of the purge test for four joint sampling locations is shown in figures 21(a) to (d). The gaseous-nitrogen concentrations obtained at the butt joints for tests 12-1 and 13 indicated approximately the same rate of reduction in nitrogen concentration as that obtained in the earlier purge tests conducted (ref. 4) for similar helium purge conditions. The data for the remaining purge tests shown in figures 21(a) to (d) indicate that the nitrogen concentration at the butt joint was reduced at a somewhat slower rate, although the difference is slight for the lower cone - gore panel butt joint (fig. 21(d)). The reason for this is not known specifically, but it is believed to be due to some slight shifting of the insulation panels as the insulation is subjected to the repeated purge, pumpdown, and repressurization cycles during the experimental tests. Any shifting of the MLI panels could cause variations in the width of the gap at the butt joints between the edges of the panels. This could affect the flow of purge gas through the butt joint and,

therefore, influence the rate of reduction of nitrogen concentration (ref. 8). There was also a shorter time interval between the points when gas samples were obtained for tests 12-1 and 13. It is believed that this did not influence the measured gaseous nitrogen concentrations, however, since they have been previously shown to be unaffected by gas sampling intervals ranging from 20 minutes to 1 hour for the type of gas sampling system utilized (refs. 8 and 9). The faired curves drawn through the bulk of the data in figures 21 (a) to (d) were used as the boundary conditions at the edges of the MLI panels to predict the gaseous nitrogen concentrations within the MLI panels. Typical times required to reduce the gaseous nitrogen concentrations to 1 percent at the butt joints were 147 minutes for the upper and lower cone - gore panel butt joints, 132 minutes for the butt joint at the upper half of the gore panel, and 114 minutes for the butt joint at the lower half of the gore panel. No data were obtained at the butt joints for test 10-1 because the thermal conductivity cell used to measure those gas concentrations was inoperative for that test.

The measured gaseous-nitrogen concentrations at four of the gas sampling locations within the MLI panels are shown in figures 21(e) to (h). These data indicate the same trends as already noted by the data for the butt joints. Typical times required to obtain 1-percent-gaseous-nitrogen concentrations, for the bulk of the data, ranged from approximately 120 minutes near the top of the tank to approximately 170 minutes near the bottom of the tank. The curves drawn in figures 21(e) to (h) are predicted gaseous-nitrogen concentrations obtained using the analytical computer program described in reference 4 along with the boundary conditions noted earlier for figures 21(a) to (d). The value of the diffusion coefficient used was obtained from reference 9. The predicted rate of reduction in gaseous-nitrogen concentration was somewhat slower than that measured for the MLI sampling points for the upper half of the tank; this is due to the natural bouyancy of the gaseous helium promoting an upward flow toward the top of the tank within the MLI panels that is not accounted for in the analytical program. For the MLI on the lower half of the tank, the measured and predicted concentrations agreed fairly well.

Ground-hold thermal performance. - The measured and predicted ground-hold thermal performance of the insulation system is shown in figure 22. The measured heat input attributed directly to the MLI for most of these tests was approximately 4000 watts (13 700 Btu/hr), although the heat input decreased to approximately 3600 watts (12 300 Btu/hr) for test 13. The amount of liquid hydrogen in the test tank varied somewhat from test to test; however, the liquid surface was generally in the vicinity of the PRT located at the 5.19-percent ullage level. The PRT located at the 1.50-percent ullage level always indicated it was in gaseous hydrogen, while the PRT located at the 6.50-percent ullage level indicated that it was always immersed in liquid hydrogen. The liquid level was above the 5.19-percent ullage level for tests 10-2 and 10-5 to 13.

The change in boiloff flow-rate measurement devices from a venturi to a flat-plate orifice provided no difference in the measured flow rate. The predicted ground-hold thermal performance, based on measured insulation temperatures and gaseous-helium thermal conductivity, remained at approximately 4750 watts (16 200 Btu/hr).

The measured insulation temperature profiles obtained during ground-hold conditions for several of the tests are shown in figure 23. The temperatures on the upper cone were considerably warmer and tended to vary somewhat more from test to test than the temperatures for the gore panel and lower cone. The warmer temperatures were most probably caused by the natural convection of the helium purge gas rising toward the top of the upper cone. The discontinuity in the faired curve for the lower cone is most probably caused by the existence of a separation between the inner and outer blankets of MLI due to the technique of mounting the insulation system on the test tank. The temperatures shown for the gore panels represent averages of the temperatures at the three locations on the centerline of individual gore panels; these temperatures showed very little variation with location.

Transient heat input. - The heat input to the test tank attributed to the MLI during the transition from ground-hold to space-hold vacuum conditions is shown in figure 24 for test 11-3, which is typical of all the tests in this series (data for test 16-2 will be discussed later). The heat input reached a minimum value 4 to 6 hours after the start of the vacuum chamber pumpdown because of the decrease in the insulation temperatures (fig. 19) caused by venting the cold helium purge gas adjacent to the tank wall. The heat input increased as the insulation warmed up and reached a steady-state value approximately 45 hours after the start of the vacuum chamber pumpdown.

Space-hold thermal performance. - The measured heat inputs to the test tank during the steady-state portions of the space-hold thermal performance tests are tabulated in table VII. The one exception is test 10-1 for which steady-state conditions were not achieved. The miscellaneous heat inputs as well as those for the tank support struts and Nylon positioning pins remained relatively constant from one test to the next. The vacuum levels measured within the shroud were sufficiently low such that gaseous conduction through the insulation should not be a significant mode of heat transfer. The resulting heat input to the test tank attributed to the MLI alone is tabulated in table VII and is also plotted in figure 25. In general, the MLI heat input tended to steady out at 7.50 watts (25.6 Btu/hr) as typified by test 13, for example. The space-hold thermal performance was not significantly affected by (1) thermal cycling, (2) the addition of the repressurization sequence to simulate the complete thermal cycle (test 11), (3) the change in insulation temperatures during purging from 344 to 300 K (620° to 540° R) (test 12), or (4) the repressurization sequence utilizing gaseous nitrogen rather than gaseous helium to repressurize the vacuum chamber (test 12-2).

Repressurization. - The repressurization sequence utilizing gaseous nitrogen for

the vacuum chamber repressurization had already been demonstrated to be ineffective in maintaining low concentrations of nitrogen within the MLI system with the test tank and MLI at ambient temperature (ref. 4). This repressurization sequence was attempted once more in this series of tests with the test tank walls cold (≈111 K (200° R)) and with the insulation temperatures varying between 88 and 262 K (158° and 472° R) (test 12-2). The gaseous-nitrogen concentration within the MLI system at the end of the repressurization sequence varied from 78 to 60 percent. While the gaseous-helium flow under the MLI system during the repressurization did not prevent gaseous nitrogen (and presumedly water vapor if it had also been present) from entering the MLI system, no degradation to the subsequent space-hold thermal performance of the insulation system (test 13) was noted.

Degradation Due to Moisture (Tests 14 to 17)

The purpose of this series of tests was to determine if moisture (water) introduced into the vacuum chamber and MLI system prior to purging the MLI would degrade the space-hold thermal performance of the insulation. Approximately 100 cubic centimeters (6.1 $in.^3$) of water, depending on the assumed temperature of the vacuum chamber and MLI system, was calculated to be sufficient to provide a 100-percent relative humidity environment within the vacuum chamber. For this series of tests, the vacuum chamber was initially backfilled with gaseous nitrogen, or gaseous helium (test 16), from vacuum conditions to approximately 7×10^4 newtons per square meter (10 psia). The water was then introduced into the vacuum chamber, and the resulting environmental pressure within the chamber was maintained until just prior to starting the purge test when the chamber pressure was increased to a 1-atmosphere pressure with gaseous nitrogen or helium (table IV).

For test 14-1, the water was intended to be added in the form of vapor through the MLI purge tubing by heating the water in a closed metal container connected to the MLI purge manifold. However, when the metal container was disconnected after the purge test had been started, it was found that very little, if any, water had been introduced into the MLI system and vacuum chamber. For test 14-2, it was intended initially to add 150 cubic centimeters (9.2 $in.^3$) of liquid water through the MLI purge tubing. This time, however, the water apparently froze in the MLI purge manifold and blocked the small diameter purge orifices after an undetermined amount of water had been added to the vacuum chamber. An additional 150 cubic centimeters (9.2 $in.^3$) of water were then added through the chamber vent line near the bottom of the vacuum chamber. For tests 15-1 to 17-1, all the water was added through the chamber vent line. For test 17-2, the chamber was backfilled to a 1-atmosphere pressure and an open container of water was placed on top of the shroud through a service port in the chamber lid. The insula-

tion was exposed to the 100-percent relative humidity environment for approximately 2 hours before purging for tests 14-2 to 16.1 (table IV). For tests 16-2 to 17-2, the exposure time was increased to as long as 8 weeks.

Purge test results. - The purge test results for those tests in which the vacuum chamber was initially backfilled with gaseous nitrogen (tests 14-1 to 15-2 and tests 17-1 and 17.2, table IV) are shown in figure 26. The data for the boundary conditions at the butt joints are shown in figures 26(a) to (d). Although the data again show a considerable amount of variation from one test to the next, the results do not, in general, differ significantly from those already shown for previous tests (fig. 21). The exceptions are for the sampling locations on the lower half of the tank for test 14-2, which shows a considerably slower rate of decrease in the nitrogen concentration than previously, particularly for the last half of the purge test. This may be due to the two purge orifices being at least partially blocked by frozen water which may have still existed in the MLI purge manifold for this particular test. The data for test 15-2 are shown by means of double symbols; the first symbol being the indicated nitrogen concentration after 60 seconds of flow through the sampling tube, and the flagged symbol being the indicated concentration after an additional 15 seconds of flow. These data confirmed that the additional 15 seconds of sampling time did not significantly influence the measured results. The faired curves drawn through the data for the slowest and the fastest rates of reduction in nitrogen concentration (tests 14-2 and 15-1, respectively) were used as inputs to the analytical computer program to predict the resulting concentration within the MLI panels.

The measured nitrogen concentrations within the MLI panels are shown in figures 26(e) to (h) along with the calculated concentrations for tests 14-2 and 15-1. The experimental data, in general, reflect the trends established by the nitrogen concentrations at the adjacent butt joints. The variation in data from test to test, therefore, is believed to be real and simply reflects the varying purge characteristics of the insulation system as it is subjected to repeated thermal and pumpdown - repressurization cycles. The calculated concentrations agree with the experimental data reasonably well except where the buoyancy of the helium purge gas aided the purge process on the upper half of the tank.

Ground-hold thermal performance. - The measured and predicted ground-hold thermal performance of the insulation system for tests 14-1 to 17.2 is shown in figure 22. The measured heat input attributed to the MLI averaged approximately 3600 watts (12 300 Btu/hr) for these tests. The measured heat input of about 3000 watts (10 200 Btu/hr) for test 16-1 was considerably lower than for the other tests; the reason for this is not specifically known. The predicted heat input for these tests tended to remain at approximately 4750 watts (16 200 Btu/hr) except for tests 16-1 and 17-2 for which it was somewhat higher. This was due to a somewhat higher overall temperature

difference across the insulation as indicated in figure 23 for test 16-1. No predicted ground-hold heat input was available for test 16-2 (fig. 22) because the required digital high-speed data was lost.

MLI temperature history. - The MLI temperature history during one of the tests (i.e., test 16-2) in this series in which moisture had been added to the vacuum chamber is shown in figure 27 starting with the vacuum chamber pumpdown. The temperature history for test 11-3 where no moisture had been added is also shown for comparison. For test 16-2, the insulation had been subjected to a 100-percent relative humidity environment for 65 hours prior to starting the ambient temperature purge test (table IV). An initial gaseous-helium background was used for this test, and the helium purge of the insulation was continued for only 1 hour so that the effect of a relatively large amount of moisture remaining within the MLI system could be determined. The major effect on the MLI temperature history was the rapid rise of the intermediate cover sheet temperature to a level higher than the normal steady-state space-hold value shorter after the vacuum chamber was pumped down to vacuum conditions. This was probably due to a high rate of outgassing of water vapor in the outer MLI blanket and perhaps the outer layers of the inner MLI blanket. The increased outgassing would cause a higher interstitial pressure within the MLI blankets which would provide a relatively high gaseous conduction heat-transfer rate between radiation shields in these portions of the MLI blankets. The higher rate of heat transfer would tend to lower the outside surface temperature of the insulation (where heat transfer would still be primarily by radiation alone) while elevating the temperatures within the insulation system. As the outgassing rate decreased because of the diminishing amounts of water vapor remaining within the MLI blankets, the outer and intermediate cover sheet temperatures gradually approached their normal steady-state values of approximately 299 and 217 K (539° and 391° R), respectively.

During the transition to steady-state conditions, it was noted that the vacuum chamber and shroud vacuum levels would fluctuate erratically from time to time indicating temporarily high outgassing rates that would tend to overpower the vacuum pumps. The temperature fluctuations of the inner cover sheet, in particular, were apparently due to the sporadic outgassing of the absorbed or frozen water vapor and the resultant fluctuations in vacuum level within the vacuum chamber. As the space-hold test continued, the fluctuations in the vacuum level became less pronounced, and a fairly steady vacuum level was present during the last 1 to 2 days of the test.

The temperature history shown for test 16-2 in figure 27 is typical of tests 14-2 to 17.2. The MLI temperature history for test 14-1 was similar to that shown for test 11-3 in that it indicated no significant amounts of water vapor had been added to the vacuum chamber prior to starting test 14-1 by the technique utilized for that particular test.

Transient heat input. - The effect of the residual water vapor outgassing within the

MLI system and the resulting elevated MLI temperatures on the heat input into the test tank attributed to the MLI during the transition to steady-state space-hold conditions for test 16-2 is shown in figure 24. The heat input remained at a value of approximately 14 watts (48 Btu/hr) for a period of several hours while the intermediate cover sheet temperature reached its maximum value and started to decrease. The heat input then decreased and reached its steady-state space-hold value approximately 60 to 65 hours after the start of the vacuum chamber pumpdown.

Space-hold thermal performance. - The measured heat inputs into the test tank during the steady-state portions of the space-hold thermal performance tests for this series of tests, as well as those from reference 4, are tabulated in table VII. The resulting heat input to the test tank attributed to the MLI is also tabulated in table VII and is plotted in figure 25. The thermal performance of the insulation for test 14-1 was not degraded at all from the previous values; this is another indication that no water vapor actually got into the vacuum chamber. For the remaining tests, some degradation in the thermal performance of the insulation was noted. However, the amount of degradation ranged from only 5.5 to 18.8 percent of the nominal heat input of 7.50 watts (25.6 Btu/hr) for test 13. Since the range of the experimentally measured thermal performance of even flat samples of DAM/silk net insulation (as well as other MLI systems) may vary as much as ±10 percent from the predicted performance (ref. 5), the degradation in thermal performance due to the presence of water vapor observed in this investigation does not seem to be particularly significant. Neither the time duration of the helium purge nor the purge gas temperature appeared to have any significant effect on the degree of thermal degradation. There was some indication that longer exposure times to water vapor (tests 16-2 to 17-2) tended to increase the degree of thermal degradation, but it was not conclusive.

Final Space-Hold Thermal Performance (Test 18)

A final space-hold thermal performance test (test 18) was conducted to determine if the previous exposure of the insulation system to the water vapor had resulted in any permanent damage to the MLI. The vacuum chamber was pumped down and the insulation was exposed to a vacuum environment at ambient temperature for 5 days to remove any residual water vapor from the MLI prior to filling the test tank with liquid hydrogen. The resulting heat input attributed to the MLI (tables V and VII and fig. 25) was 8.04 watts (27.5 Btu/hr). This was only 7.2 percent greater than the nominal thermal performance of 7.50 watts (25.6 Btu/hr) achieved for test 13 prior to the thermal degradation tests. It was also lower than at least one previous space-hold thermal performance test (test 10-5) and was very close to the predicted performance of 7.98 watts

(27.2 Btu/hr) for test 13 as noted in table V. It was concluded, therefore, that little if any permanent damage to the insulation system resulted as a consequence of the exposure to a 100-percent relative humidity environment.

Posttest Inspection of MLI System

During the conduct of the complete test program (tests 1 to 18), the insulated test tank was installed in the vacuum chamber for just over 1 year without being removed. After the test program had been completed, the test tank was removed from the vacuum chamber, and the insulation system was inspected visually. The exterior surface of the insulation appeared to be coated with a very light film of diffusion pump oil; all other surfaces within the vacuum chamber appeared to be clean and dry. All of the Velcro fastener material checked was still mated and holding. Almost all of the aluminized Mylar tape was still well bonded adhesively to the surfaces to which it was attached. The gas sampling tubes were still in the proper locations. No structural damage of any sort to the insulation system was noted.

The emissivity of several of the radiation shields in two of the MLI panels was checked with the Gier Dunkle reflectometer. For 25 readings taken on the aluminized Mylar radiation shields the average total hemispherical emissivity was 0.050, which indicated that no degradation of the MLI system due to exposure to water vapor had occurred. The aluminized surfaces of the radiation surfaces still appeared bright and shiny; no peeling of the aluminizing from the Mylar plastic film was observed.

CONCLUDING REMARKS

A comparison of the two reusable insulation systems reported in references 2 and 3 with the insulation system tested in this investigation is tabulated in table VIII. The DGK/Dacron tuft MLI system (ref. 2) reportedly gave excellent thermal performance (0.60 W/m^2 (0.19 $Btu/hr\text{-}ft^2$)), but it suffered from weight penalties (3.71 $kg\text{-}W/m^4$ (0.241 $lbm\text{-}Btu/hr\text{-}ft^4$)) due to using the fiberglass tank fairings and purge bag. The thermal performance of the two DAM/silk net MLI systems ($\approx$1.38 W/m^2 (0.438 $Btu/hr\text{-}ft^2$)) was about equal. Both were poorer than that of the DGK/Dacron tuft MLI system, although the DAM/silk net system was more efficient when the weight of the system was included (2.37 to 2.68 $kg\text{-}W/m^4$ (0.154 to 0.174 $lbm\text{-}Btu/hr\text{-}ft^4$)). The DGK/Dacron tuft MLI system would be difficult to apply to a double-contoured tank surface (except for perhaps a large tank) because of the difficulties that would be encountered in folding (or cutting) and taping the radiation shields to conform to the tank surface. The use of the silk netting as a spacer material allows the forming to be readily accomplished.

The trade-off between the two MLI systems, therefore, is really the better thermal performance of the DGK/Dacron tuft system as against the potentially lower cost and ease of fabrication of the DAM/silk net system, assuming they both meet all other requirements.

It also appeared that certain improvements could be made in the MLI system reported in this investigation to improve its basic thermal performance. These potential improvements include the following:

(1) Eliminate the Nylon positioning pins and grommets at the equator of the tank

(2) Revise the insulation system configuration near the top and bottom of the tank so that the positioning pins located there do not penetrate the MLI panels

(3) Eliminate the Y-type MLI panel joint between the conical MLI panels and the gore panels for the inner MLI blanket and use instead the more conventional butt joint configuration

(4) Use a better technique for installing the insulation around the tank support brackets and struts (such as noted in refs. 10 and 11, e.g.)

(5) Reduce the seam or butt joint length

In regard to the last item, the seam length could be decreased by reducing the number of gore panels in a given MLI blanket or by changing the gore panel half-angle θ_g. The seam length can be calculated for half the propellant tank from

$$\ell_s = \pi r_{MLI}\left[n\left(\frac{\theta_g}{180}\right) + 2\cos\theta_g\right] \tag{6}$$

The results are shown in figure 28 for the particular size test tank and insulation thickness used in this test program. The number of gore panels per MLI blanket could have been reduced from 6 to 4 and still have stayed within the limitations imposed by the maximum width of the insulation materials available. Also, the gore panel half-angle θ_g could have been increased somewhat (perhaps from 45^o to 50^o, e.g.). These modifications to the insulation system would have reduced the total seam length for half the tank from 6.56 to 5.39 meters (21.5 to 17.7 ft). The total heat input into the test tank then would have been reduced by 0.40 watt (1.35 Btu/hr), a reduction of about 5.3 percent from the nominal MLI heat input of 7.50 watts (25.6 Btu/hr) for test 13.

A second possible technique for reducing the seam length would be to leave the gore panel half-angle θ_g fixed and to increase the length of the gore panels to extend part way up the conical sections. For this case, the seam length for half the tank can be determined from

$$\ell_s = n\left[\pi r_{MLI}\left(\frac{\theta_g}{180}\right) + \frac{x}{\cos\theta_g}\right] + 2\pi(r_{MLI}\cos\theta_g - x\tan\theta_g) \tag{7}$$

The results are shown in figure 29 for the current test tank and a gore panel half-angle θ_g of 45^o. In this case, the seam length can be reduced only by reducing the number of MLI gore panels per blanket to four. Using any larger number only results in increasing the total seam length as the gore panels are extended up on the conical section.

The heat input into the upper half of the test tank attributed to the MLI, considering the different heat fluxes through the MLI for the gore panels and conical panels as well as the thermal degradation due to the seams, can be predicted from

$$Q_{MLI} + Q_s = A_g\dot{q}_g + A_{co}\dot{q}_{co} + \ell_s q_s \tag{8}$$

where ℓ_s is determined from equation (6) and

$$A_g = 2\pi r_{MLI}^2 \sin\theta_g$$

$$A_{co} = \pi\left[r_a^2 + \frac{\left(r_{MLI}\cos\theta_g\right)^2 - r_a^2}{\sin\theta_g}\right]$$

The predicted heat input to the upper half of the test tank as a function of the number of gore panels per blanket and the gore panel half-angle θ_g is shown in figure 30 for the following heat fluxes:

$$\dot{q}_g = 0.492\ W/m^2\ (0.156\ Btu/hr\text{-}ft^2)$$

$$\dot{q}_{co} = 0.457\ W/m^2\ (0.145\ Btu/hr\text{-}ft^2)$$

$$q_s = 0.169\ W/m\ (0.176\ Btu/hr\text{-}ft)$$

Decreasing the number of gore panels per blanket, in particular, can significantly reduce the heat input into the tank. Assuming that the upper and lower halves of the tank had the same MLI system configuration and using heat inputs taken from figure 30, the total MLI system heat input into the test tank for the current MLI system would be predicted to be 8.91 watts (30.4 Btu/hr) as noted in table IX. If the number of gore panels were reduced to four, the gore panel half-angle was increased to 50^o, the thermal degradation of the MLI near the tank support struts was reduced by 50 percent, and the heat

input through the Nylon positioning pins was eliminated, the resulting predicted heat input would be 6.22 watts (21.2 Btu/hr), an improvement of 30.2 percent. All these improvements are realistic and could be realized with generally minor changes in the MLI system design.

One additional improvement in the MLI system design could be made if it was desirable to decrease the time required to purge the insulation to less than 1-percent-gaseous-nitrogen concentration and to achieve a more uniform purge gas concentration from the top to the bottom of the insulation. This would be to provide a slotted plastic purge pin at the bottom of the tank which would penetrate the lower conical MLI panels except for the outer cover sheet of the outer MLI blanket. The purge pin would be attached to the lower fiberglass cone on the longitudinal centerline of the tank. The pin would distribute the helium purge gas between the individual radiation shields. A positive flow of purge gas would be supplied through one additional purge tube. It is estimated that this would reduce the total purge time for the lower conical MLI panels by $\frac{1}{2}$ to 1 hour.

SUMMARY OF RESULTS

An experimental investigation was conducted to determine (1) the ground-hold and space-hold thermal performance of a MLI system mounted on a spherical liquid hydrogen propellant tank and (2) the degradation to the space-hold thermal performance of the MLI system that occurred as a result of both thermal cycling and moisture introduced into the insulation panels. The propellant tank had a diameter of 1.39 meters (4.57 ft). The MLI consisted of two blankets of insulation; each blanket contained 15 double-aluminized Mylar radiation shields alternated with 16 double silk net spacers. A laminated aluminized Mylar/Dacron scrim sheet was applied to each side of each blanket. The MLI system configuration used six 60°-gore MLI panels, one upper conical MLI panel, and one lower conical MLI panel in each blanket.

Nineteen tests simulating typical cryogenic spacecraft thermal (environmental) conditions were conducted. Each thermal cycle imposed on the insulation system typically consisted of either a 300 or a 344 K (540° or 620° R) temperature gaseous-helium purge, a 1-atmopshere environmental-pressure tank fill and ground-hold condition, a vacuum chamber pumpdown and vacuum space-hold condition, and a repressurization of the vacuum chamber insulation system back to a 1-atmosphere pressure condition. Prior to each of the last seven tests, water vapor was introduced into the vacuum chamber for varying periods before initiating the gaseous-helium purge to determine the subsequent effect on the space-hold thermal performance of the insulation system. The following results were obtained from this test program:

1. The initial baseline space-hold thermal performance test conducted indicated that the nominal heat input attributed to the MLI system under vacuum conditions was 7.18 watts (24.5 Btu/hr). The average heat input for the first four space-hold tests was 7.40 watts (25.3 Btu/hr) with a maximum deviation of 6 percent. This heat-transfer rate corresponded to a boiloff rate of 1.45 percent of the tank volume per day. The predicted heat input of approximately 8.00 watts (27.3 Btu/hr), calculated using the experimentally measured insulation cover sheet temperatures, was 8 percent higher than the average measured heat input.

2. The initial ground-hold heat input attributed to the MLI system was 3845 watts (13 130 Btu/hr), which was approximately 19 percent less than the predicted heat input of 4762 watts (16 260 Btu/hr) calculated using the experimentally measured cover sheet temperatures. The measured heat input corresponded to a boiloff rate of 31.4 percent of the tank volume per hour. Determining the change in the liquid hydrogen level in the tank when the normal boiling of the hydrogen was suppressed indicated that the apparent liquid hydrogen density under ground-hold high-heat-flux boiling conditions was 64.4 kilograms per cubic meter (4.02 lb/ft^3).

3. Typical times required to purge the initial condensible (nitrogen) gas from within the MLI panels with helium to achieve a 1-percent-gaseous-nitrogen concentration ranged from approximately 120 minutes near the top of the tank to approximately 170 minutes near the bottom of the tank. The experimental purge times required to achieve 1-percent gaseous nitrogen sometimes varied from test to test. This was thought to be a result of changing purge conditions and not a result of instrumentation error or measurement technique.

4. During the pumpdown of the vacuum chamber, the temperatures of the intermediate and outer insulation cover sheets on the gore panels initially decreased from their normal ground-hold values of approximately 145 and 215 K (261° and 387° R), respectively, to approximately 80 and 140 K (144° and 252° R). The insulation panels were chilled down by the cold helium purge gas adjacent to the tank wall venting through the insulation when the vacuum chamber was pumped down.

5. Without the presence of water vapor within the insulation systems, the transition from the pumpdown to space-hold steady-state conditions was characterized by a rapid increase in the outer cover sheet temperature and a gradual increase in the intermediate cover sheet temperature to their final steady-state values of approximately 299 and 227 K (539° and 409° R), respectively. The liquid-hydrogen boiloff rate initially decreased and then gradually increased to its final space-hold steady-state value. The boiloff rate achieved its steady-state value approximately 48 hours after the vacuum chamber was pumped down, while the intermediate cover sheet temperatures required approximately 60 hours to reach steady state. Neither the initial purge temperatures of 300 or 344 K (540° or 620° R) nor the thermal cycles imposed on the insulation system

influenced the resulting space-hold thermal performance to any discernable degree. The insulation system heat input at the end of this series of tests settled out at approximately 7.50 watts (25.6 Btu/hr) during space-hold vacuum conditions.

6. For the tests where water had been added to the vacuum chamber to provide 100-percent relative humidity conditions prior to the start of the test, the transition from the pumpdown to space-hold steady-state conditions was characterized initially by a fairly rapid increase in both the outer and intermediate cover sheet temperatures. This was followed by a gradual decrease in the intermediate cover sheet temperature to its final steady-state value of approximately 217 K (391° R). Also, the liquid-hydrogen boiloff rate was observed to gradually decrease to its final space-hold steady-state value. These changes in the transition to steady-state conditions from that noted previously for the tests without exposure to water vapor were apparently due to outgassing of water vapor in the insulation blankets causing a higher initial heat flux. However, the times for both the insulation temperature and liquid-hydrogen boiloff to reach steady-state values were approximately the same as noted previously for the tests without water vapor. The presence of the water vapor resulted in MLI space-hold heat inputs as high as 8.91 watts (30.4 Btu/hr), which is approximately 19 percent higher than the nominal values obtained in the previous tests without water vapor.

7. The variation in purge temperatures from 300 to 344 K (540° to 620° R) caused little effect in the resulting space-hold thermal performance and apparently was not effective in removing additional amounts of water vapor from within the insulation system Shorter purge times and longer initial exposure times apparently allowed some increased amounts of water vapor to remain in the insulation system after purging and resulted in somewhat increased insulation heat inputs during space-hold vacuum conditions.

8. The final space-hold thermal performance test indicated that the heat input attributed to the MLI system had been restored to 8.04 watts (27.5 Btu/hr). This was very close to the predicted heat input of 7.98 watts (27.2 Btu/hr) and was only 7.2 percent greater than the nominal space-hold thermal performance of 7.50 watts (25.6 Btu/hr).

9. A posttest inspection of the MLI system revealed that no structural damage had occurred as a result of the purge, pumpdown, and repressurization conditions imposed. In addition, no degradation of the emissivity of the radiation shields was measured.

10. It appears that improvements could be made in the insulation system configuration tested to reduce the space-hold heat input into the liquid-hydrogen propellant tank. Changes in the MLI system configuration, such as elimination of the Nylon positioning pins, reduction of the number of gore panels per blanket from 6 to 4, increase in the gore panel half-angle from 45° to 50°, and change in the technique of insulating around the tank support struts to provide a 50-percent reduction in the degradation of the MLI due to the penetration of the tank support brackets and struts, could result in a reduction

of the total heat input from 8.91 watts (30.4 Btu/hr) that was measured for test 13 (typical of the thermal cycle tests) to 6.22 watts (21.2 Btu/hr), a decrease of 30.2 percent.

Lewis Research Center,
National Aeronautics and Space Administration,
Cleveland, Ohio, March 14, 1978,
506-21.

REFERENCES

1. Baseline Space Tug System Requirements and Guidelines. MSFC 68M00039-1, George C. Marshall Space Flight Center, July 15, 1974.
2. Walburn, A. B.: Development of a Reusable Flightweight Cryogenic Storage System. AIAA Paper 74-726, July 1974.
3. Knoll, Richard H.; and DeWitt, Richard L.: Thermal Performance of a Modularized Replaceable Multilayer Insulation System for a Cryogenic Stage. NASA TN D-8282, 1977.
4. Sumner, Irving E.: Purging of a Tank-Mounted Multilayer Insulation System by Gas Diffusion. NASA TP-1127, 1978.
5. Keller, C. W.: Cunnington, G. R.; and Glassford, A. P.: Thermal Performance of Multilayer Insulations. (LMSC-D349866, Lockheed Missiles and Space Co.; NASA Contract NAS3-14377.) NASA CR-134477, 1974.
6. Sumner, Irving E.: Degradation of a Multilayer Insulation Due to a Seam and a Penetration. NASA TN D-8229, 1976.
7. Space Tug Point Design Study. Volume II: Operations, Performance and Requirements. (SD72-SA-0032, vol. 2, North American Rockwell Corp.; NASA Contract NAS7-200.) NASA CR-120110, 1973.
8. Sumner, Irving E.; and Fisk, William J.: Purging of a Multilayer Insulation with Dacron Tuft Space by Gas Diffusion. NASA TM X-3456, 1976.
9. Sumner, Irving E.; and Spuckler, Charles M.: Purging of Multilayer Insulation by Gas Diffusion. NASA TN D-8122, 1976.
10. Krause, D. R.: Development of Lightweight Material Composites to Insulate Cryogenic Tanks for 30-Day Storage in Outer Space. (MDC G2742, McDonnell Douglas Corp.; NASA Contract NAS8-26006.) NASA CR-123828, 1972.
11. Glaser, Peter E.; et al.: Thermal Insulation Systems. A Survey. NASA SP-5027, 1967.

TABLE I. - MLI SYSTEM COMPONENT WEIGHTS

Item	Material	Unit weight
Cover sheet	Reinforced Mylar laminate, aluminized both sides (0.0064-mm Mylar - Dacron scrim - 0.013-mm Mylar)	78.9 g/m^2
Spacer	Silk net, single thickness (4.7×7.1 mesh/cm^2)	6.5 g/m^2
Radiation shield	0.0064-mm double-aluminized Mylar	9.5 g/m^2
Button-pin studs	Nylon	0.1 g each
Velcro fastener	Polyester, 2.5 cm wide (average value for hook or pile sections)	10.7 g/m
Velcro fastener	Polyester, 5,1 cm wide (average value for hook or pile sections)	31.5 g/m
Grommet	Nylon	0.8 g each
Positioning pins	Nylon with Teflon washer and stainless-steel hitch pin	3.0 g each
Ideal MLI panel	2 cover sheets, 16 double silk net spacers, 15 radiation shields, and 25 button-pin studs/m^2	0.511 kg/m^2

TABLE II. - MLI SYSTEM WEIGHT BREAKDOWN

Item	Calculated weight, kg							Actual weight, kg
	DAM	Silk net	Cover sheets	Grom-mets	Button-pin studs	Velcro fastener	Total	
Upper conical MLI panels:								
Inner blanket	0.105	0.152	0.116	-----	0.004	0.015	0.39	0.38
Outer blanket	.154	.224	.170	-----	.004	.008	.56	.56
MLI 60^o gore panels:								
Inner blanket	.756	1.100	.878	0.031	.022	.110	2.90	3.13
Outer blanket	.637	.927	.815	.010	.018	.090	2.50	3.00
Lower conical MLI panels:								
Inner blanket	.109	.159	.121	-----	.003	.024	.42	.44
Outer blanket	.160	.233	.177	-----	.004	.017	.59	.60
Positioning-pin covers:								
Large rectangular (3)	.020	.033	.067	-----	-----	.006	.13	.14
Small circular (6)	.005	.009	.017	-----	-----	.003	.03	.04
Tank wall Velcro pile	-----	-----	-----	-----	-----	.088	.09	(.09)
Nylon positioning pins	-----	-----	-----	-----	-----	.110	.11	(.11)
Total MLI	-----	-----	-----	-----	-----	-----	7.72	8.49
Fiberglass cones:								
Upper cone and brackets	-----	-----	-----	-----	-----	-----	----	1.56
Lower cone and brackets	-----	-----	-----	-----	-----	-----	----	1.30

TABLE III. - PREVIOUS TEST HISTORY OF MLI SYSTEM (REF. 4)

Test	Type of test	Ground-hold purge conditions							Space-hold MLI thermal performance		Repressurization		
		MLI			Chamber						Purge gas		Time required, min
		Gaseous helium purge rate		Heater temperature, K	Gas	Purge rate		Shroud temperature, K	W	Btu/hr	MLI	Chamber	
		kg/hr	vol/hr			kg/hr	vol/hr						
1	SHTP[a]	----	----	---	--------	----	----	300	7.18	24.5	------	--------	--
2A	Purge	(b)	(b)	299	Helium	(b)	(b)	↓	----	----	------	--------	--
2B	↓	0.30	10.1	↓	↓	2.13	2.37	↓	----	----	------	--------	--
2C	↓	.60	20.2	↓	↓	2.15	2.39	↓	----	----	------	--------	--
2D-1	↓	1.10	36.8	↓	↓	2.14	2.35	↓	----	----	------	--------	--
2D-2	↓	↓	36.8	↓	↓	2.15	2.36	↓	----	----	------	--------	--
2E-1	↓	↓	36.6	↓	Nitrogen	7.23	1.13	↓	----	----	------	--------	--
2E-2	↓	↓	36.8	↓	Helium	1.03	1.13	↓	----	----	------	--------	--
3	SHTP	----	----	---	--------	----	----	↓	7.33	25.0	------	--------	--
4A	Purge	1.10	36.7	299	Helium	2.14	2.35	301	----	----	Helium	Helium	38
4B	Purge	1.10	37.1	299	Helium	2.13	2.37	301	----	----	Helium	Nitrogen	49
5	SHTP	----	----	---	--------	----	----	300	7.86	26.8	------	--------	--
6A	Purge	.97	32.4	358	Helium	2.18	2.38	300	----	----	------	--------	--
6B	Purge	.96	36.1	359	Helium	1.84	2.38	352	----	----	------	--------	--
7	SHTP	----	----	---	--------	----	----	300	7.23	24.7	------	--------	--

[a]Space-hold thermal performance.

[b]Leakage of purge gas at lid of vacuum chamber precluded satisfactory test.

TABLE IV. - CURRENT TEST SEQUENCE AND TEST CONDITIONS

[MLI system volume, 0.186 m^3; vacuum chamber free volume, 5.69 m^3.]

Test	Type of test	Initial conditions			Initial purge conditions					Ground-hold gaseous helium conditions		GHTP[a] test	Pump-down	SHTP[b] test	Repressurization	Repressurization purge gas	
					MLI		Chamber									MLI	Chamber
		Chamber backfilled with -	Amount of water added, cm^3	Exposure time, hr	Gaseous helium purge rate, kg/hr	Heater temperature, K	Gaseous helium purge rate, kg/hr	Heater temperature, K	Purge time allowed, hr	MLI purge rate, kg/hr	Chamber purge rate, kg/hr						
8	GHTP	Gaseous helium	----	----	----	---	----	---	---	0.22	1.03	×				----------	----------
9	SHTP	----------	----	----	----	---	----	---	---	----	----			×		----------	----------
10-1	Thermal cycle	Gaseous nitrogen	----	----	1.10	356	2.12	339	3	.24	1.01	×	×	×		----------	----------
10-2			----	----	.96	353	1.87	351		.22	1.03	×	×	×		----------	----------
10-3			----	----	.95	353	1.83			.22	1.03	×	×	×		----------	----------
10-4			----	----	.95	353	1.83			.22	1.01	×	×	×		----------	----------
10-5			----	----	.95	352	1.85			.23	1.04	×	×	×		----------	----------
11-1			----	----	.94	353	1.84			.22	1.02	×	×	×	×	Gaseous helium	Gaseous helium
11-2			----	----	.97	353	1.92			.23	1.04	×	×	×	×		
11-3			----	----	.95	352	1.85			.22	1.01	×	×	×	×		
12-1			----	----	1.10	299	2.13	300		.30	1.03	×	×	×	×		
12-2			----	----	1.11	295	2.18	300		.31	1.05	×	×	×	×		Gaseous nitrogen
13			----	----	1.13	292	2.22	300		.31	1.06	×	×	×	×		Gaseous helium
14-1	Degradation		[c]150	2	.98	353	1.90	350		.31	1.08	×	×	×	×		
14-2			300		.99	354	1.87	350		.94	1.10	×	×	×	×		
15-1			150		1.11	295	2.15	300		.31	1.07	×	×	×	×		
15-2			300		1.12	293	2.18			.32	1.08	×	×	×	×		
16-1		Gaseous helium	300		1.12	293	2.18		1	.27	.92	×	×	×	×		
16-2		Gaseous helium	300	65	.31	293	1.11		1	.31	1.11	×	×	×	×		
17-1		Gaseous nitrogen	1000	1340	.96	354	1.85	350	4	.31	1.16	×	×	×	×		
17-2		Gaseous nitrogen	1000	120	1.09	298	2.07	300	4	.32	1.10	×	×	×	×		
18	SHTP	----------	----	----	----	---	----	---	---	----	----			×		----------	----------

[a]GHTP, ground-hold thermal performance test.

[b]SHTP, space-hold thermal performance test.

[c]Attempted to vacuum pump water vapor through MLI purge manifold. Only a trace of water vapor actually transferred into MLI system.

TABLE V. - BASIC SPACE-HOLD THERMAL PERFORMANCE DATA SUMMARY

Test	Measured heat input, W (Btu/hr)					Calculated heat input, W (Btu/hr)				
	Total into tank	Extran-eous	Tank support struts	Nylon position pins	Total through MLI	Basic gore panels	MLI cone panels	Seams	Strut degra-dation	Total through MLI
1	8.53	0.03	0.34	0.98	7.18 (24.5)	2.18	1.04	2.30	2.42	7.94 (27.1)
3	8.67	.02	↓	.98	7.33 (25.0)	----	----	----	----	----------
5	9.21	.02		.99	7.86 (26.8)	----	----	----	----	----------
7	8.59	0		1.02	7.23 (24.7)	2.24	1.04	2.30	2.42	8.00 (27.3)
9	8.14	.03		1.03	6.74 (23.0	----	----	----	----	----------
18	9.33	-.01		.96	8.04 (27.5)	2.22	1.04	2.30	2.42	7.98 (27.2)

TABLE VI. - TEST RESULTS TO DETERMINE APPARENT DENSITY OF BOILING LIQUID HYDROGEN UNDER GROUND-HOLD CONDITIONS

Initial ullage, percent	Lower PRT location, percent ullage	Time to uncover PRT, sec
5.19	6.50	10.6
	7.95	12.5
	9.51	21.9
	15.00	(a)
6.50	7.95	1.9
	9.51	4.7
	15.00	38.4

[a]Not uncovered after 80 seconds.

TABLE VII. - MLI SPACE-HOLD THERMAL PERFORMANCE

Test	Measured heat input, W				Heat input attributed to MLI, W	Hours of steady-state boiloff under desired back pressure control	Vacuum within shroud, N/m^2
	Total into tank	Miscella-neous	Tank support struts	Nylon positioning pins			
1	8.53	0.03	0.34	0.98	7.18	21	2.5×10^{-4}
3	8.67	.02	↓	.98	7.33	25	3.1×10^{-4}
5	9.21	.02		.99	7.86	40	2.2×10^{-5}
7	8.59	.00		1.02	7.23	24	2.6×10^{-4}
9	8.14	.03		1.03	6.74	24	4.5×10^{-4}
10-1	7.74	.03		1.01	6.36	(a)	4.6×10^{-4}
10-2	9.12	.01		.99	7.78	23	6.4×10^{-4}
10-3	9.00	.02		1.04	7.60	31	3.5×10^{-4}
10-4	9.36	.01		1.05	7.96	29	6.4×10^{-4}
10-5	9.63	.00		1.01	8.28	↓	3.1×10^{-3}
11-1	9.22	.01		1.05	7.82		4.0×10^{-4}
11-2	9.04	↓		1.10	7.59		3.9×10^{-4}
11-3	8.86			1.10	7.41	28	4.1×10^{-4}
12-1	8.75			1.04	7.36	28	6.4×10^{-4}
12-2	8.90			1.03	7.52	22.5	3.8×10^{-4}
13	8.88			1.03	7.50	21.5	5.1×10^{-4}
14-1	8.89			1.05	7.49	20	3.6×10^{-4}
14-2	9.68			1.05	8.28	24	6.4×10^{-4}
15-1	9.34			1.08	7.91	15	3.2×10^{-4}
15-2	9.61	.00		1.08	8.19	24	3.0×10^{-4}
16-1	9.77	-.02		1.02	8.43	24	2.0×10^{-4}
16-2	9.76	-.01		1.06	8.37	14.5	1.6×10^{-4}
17-1	10.25	-.01		1.09	8.83	46	1.5×10^{-4}
17-2	10.40	.00		1.15	8.91	20	9.6×10^{-4}
18	9.33	-.01	↓	.96	8.04	41.5	2.9×10^{-3}

[a]Did not achieve steady-state conditions during test.

TABLE VIII. - COMPARISON OF REUSABLE INSULATION SYSTEMS

	Reference 2	Reference 3	Current investigation
Radiation shield	DGK	DAM	DAM
Spacer	Dacron tuft	Silk net	Silk net
Layer density, layers/cm	11.5	17.7	17.7
Number of MLI blankets	2	2	2
Radiation shields per blanket	22	15	15
Spacers per blanket	22	16	16
Gore panels per blanket	12	6	6
Total MLI thickness, cm	3.8	1.9	1.9
Total seam length, m	39.9	20.6	13.6
Total MLI area, m^2	16.5	14.9	6.84
Tank diameter, m	2.23	2.23	1.39
Tank surface area, m^2	14.1	13.9	6.12
MLI system purge volume, m^3	2.43	Not available	0.19
Gaseous helium purge rate, MLI, vol/hr	100	----------	37
Purge time required (1-percent gaseous nitrogen), min	[a]5	----------	[b]185
Tank-mounted purge system weight, kg			
Fairings/cones	29.45	3.9	2.86
Purge bag	43.23	----------	-------
Tubing, etc.	.92	.8	.41
MLI system weight, kg	13.97	19.1	8.49
Total weight, kg	87.57	23.8	11.76
Overall thermal performance, W			
Basic MLI	3.26	[c]7.0	[d]2.78
Seams	2.76	3.9	2.30
Pins (purge/positioning)	2.43	2.0	1.03
Penetrations (fill, vent, instrument)	3.25	1.3	.01
Degradation of MLI at struts/miscellaneous	.40	6.3	2.42
Struts	.50	2.0	.34
Total (experimentally measured value)	12.60	22.5	8.88
MLI system effective thermal conductivity[e], W/m-k	7.52×10^{-5}	8.97×10^{-5}	8.49×10^{-5}
MLI system overall thermal performance[f], W/m^2	0.64	1.38	1.39
Combined thermal performance and weight criteria[g], $kg\text{-}W/m^4$	3.90	2.37	2.68

[a]Time to achieve 1-percent gaseous-nitrogen concentration at outlet of purge bag.

[b]Time to achieve 1-percent gaseous-nitrogen concentration within lower conical MLI panel (test 12-2).

[c]Test NE-1 test results.

[d]Test 13 test results.

[e][(total heat input - struts - penetrations) × insulation thickness]/(temperature difference × insulation area): For ref. 2, temperature difference (ΔT) = 291 - 20 = 271 K; for ref. 3, ΔT = 293 - 20 = 273 K; for current investigation, ΔT = 299 - 20 = 279 K.

[f](total heat input - struts - penetrations)/tank surface area.

[g][total MLI system weight × (total heat input - struts - penetrations)]/$(\text{tank surface area})^2$.

TABLE IX. - POTENTIAL IMPROVEMENT IN THERMAL PERFORMANCE OF MLI SYSTEM

Number of gore panels, n	Gore panel half angle, θ_g	Heat input, W				Improvement, percent
		Basic MLI plus seams $2(Q_{MLI} + Q_S)$	MLI thermal degradation near tank support struts	Nylon positioning pins	MLI system total	
6	45	5.46	2.42	1.03	8.91	----
4	50	5.01	1.21	----	6.22	30.2

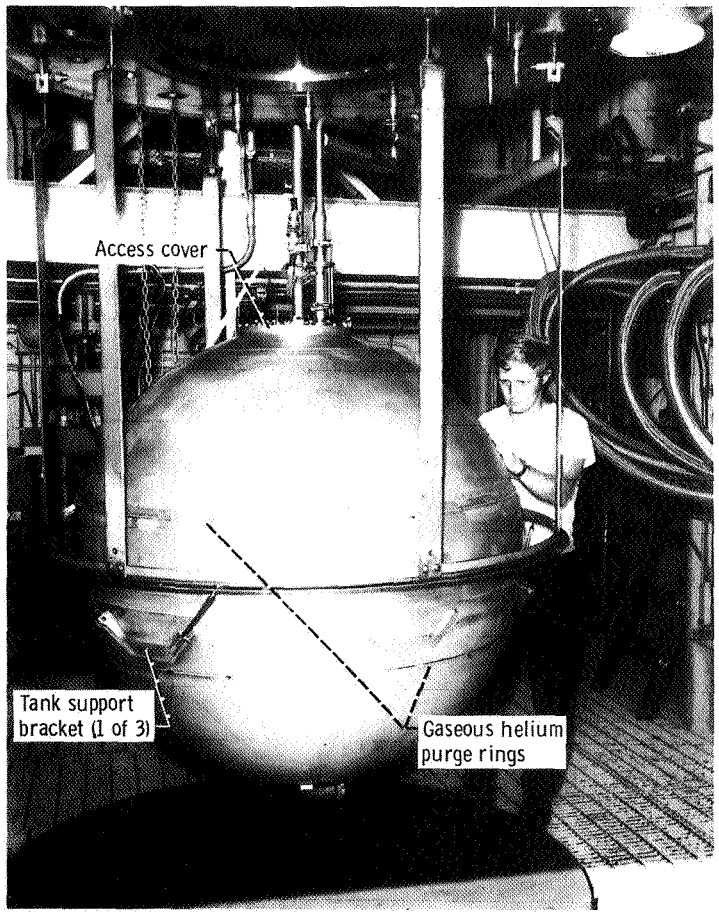

Figure 1. - Test tank.

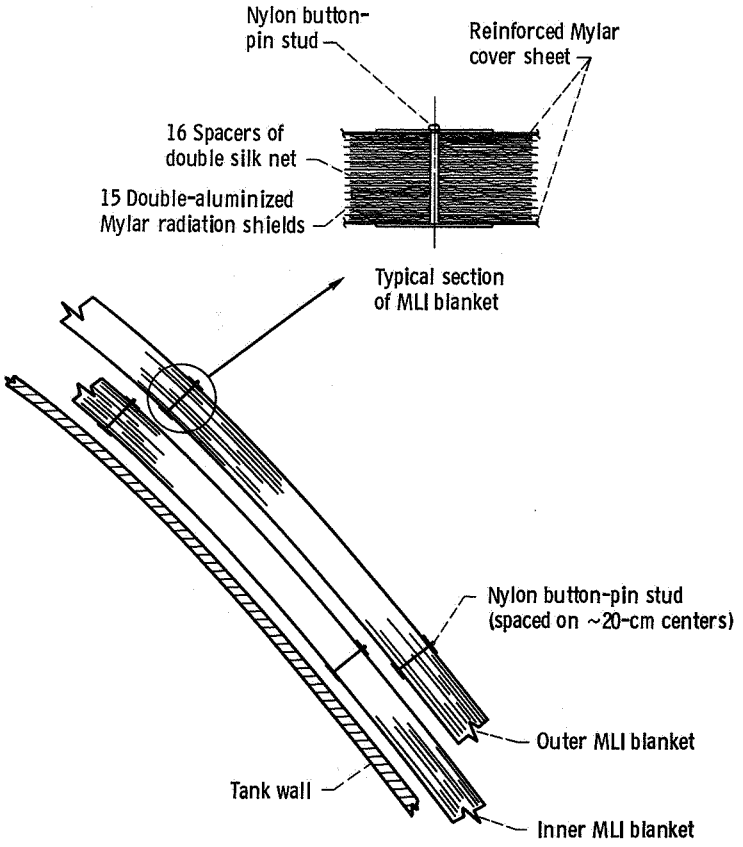

Figure 2. - Basic MLI blanket concept.

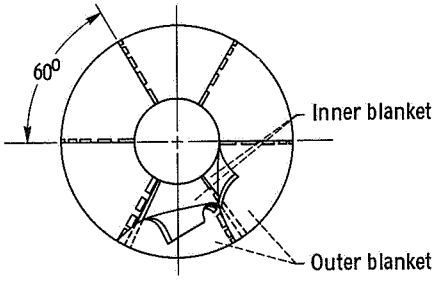

(a) Top view of tank with gore panels.

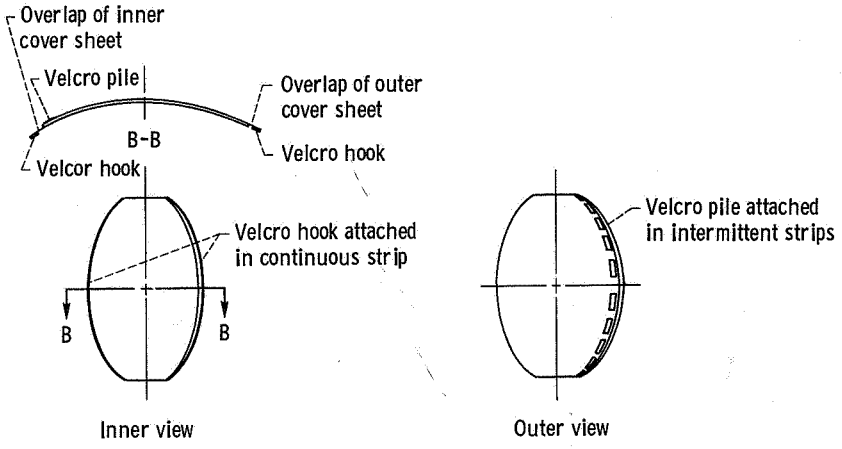

(b) Location of Velcro fastener on inner and outer cover sheets of MLI 60° gore panels.

Figure 3. - Location of Velcro fastener used to install MLI gore panels on test tank.

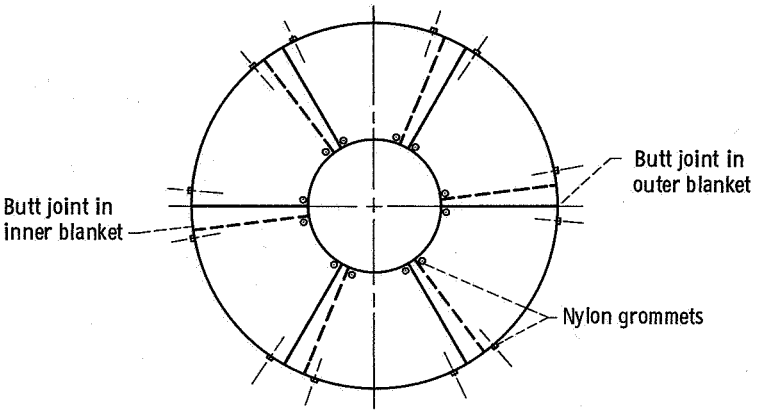

(a) Top view of tank showing grommet locations.

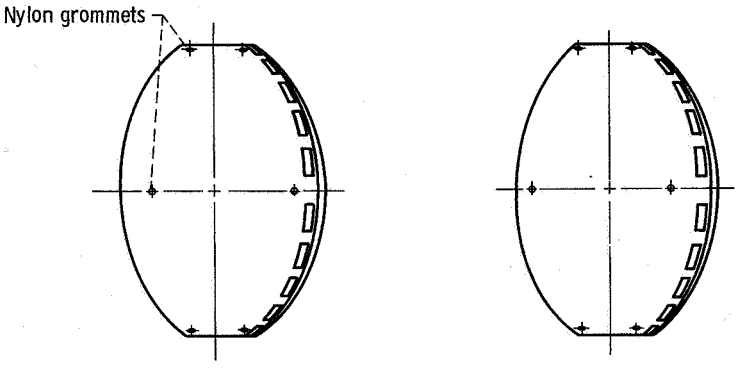

(b) Grommet locations on inner and outer MLI gore panels.

Figure 4. - Grommet locations on MLI gore panels.

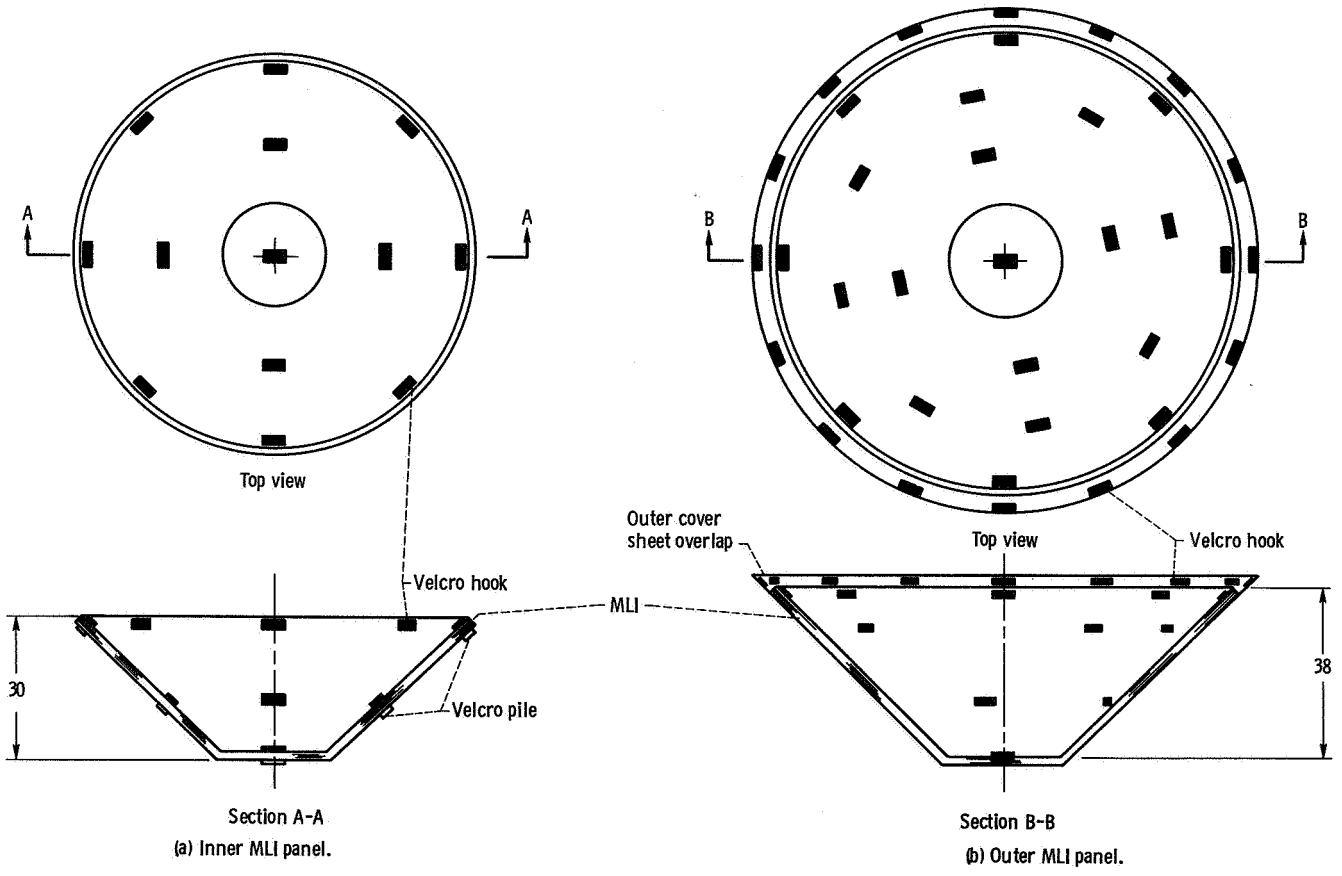

Figure 5. - General location of Velcro fastener on conical MLI panels at bottom of test tank. (All dimensions are in cm.)

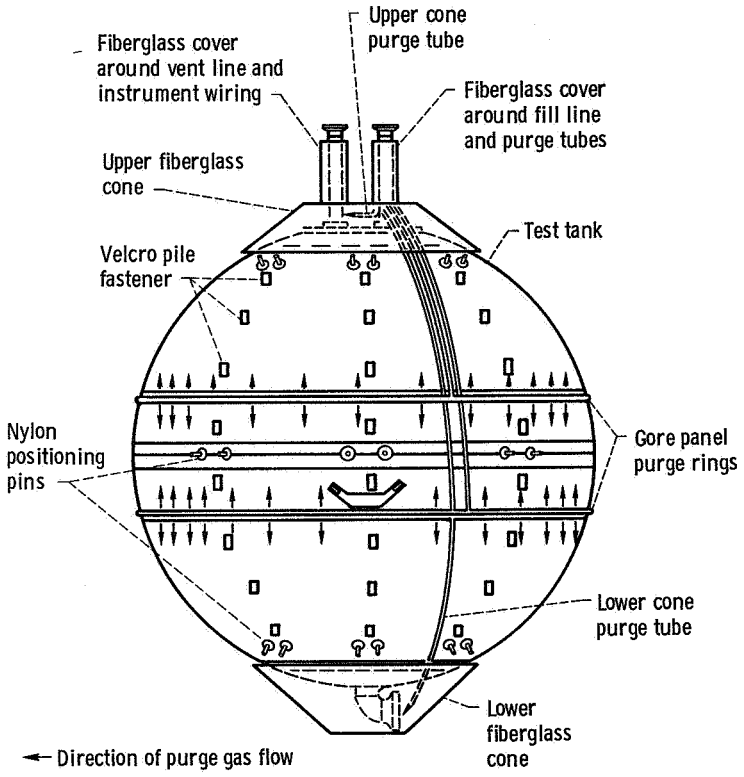

Figure 6. - Test tank showing general location of purge tubing, nylon positioning pins, fiberglass cones, and Velcro pile fastener.

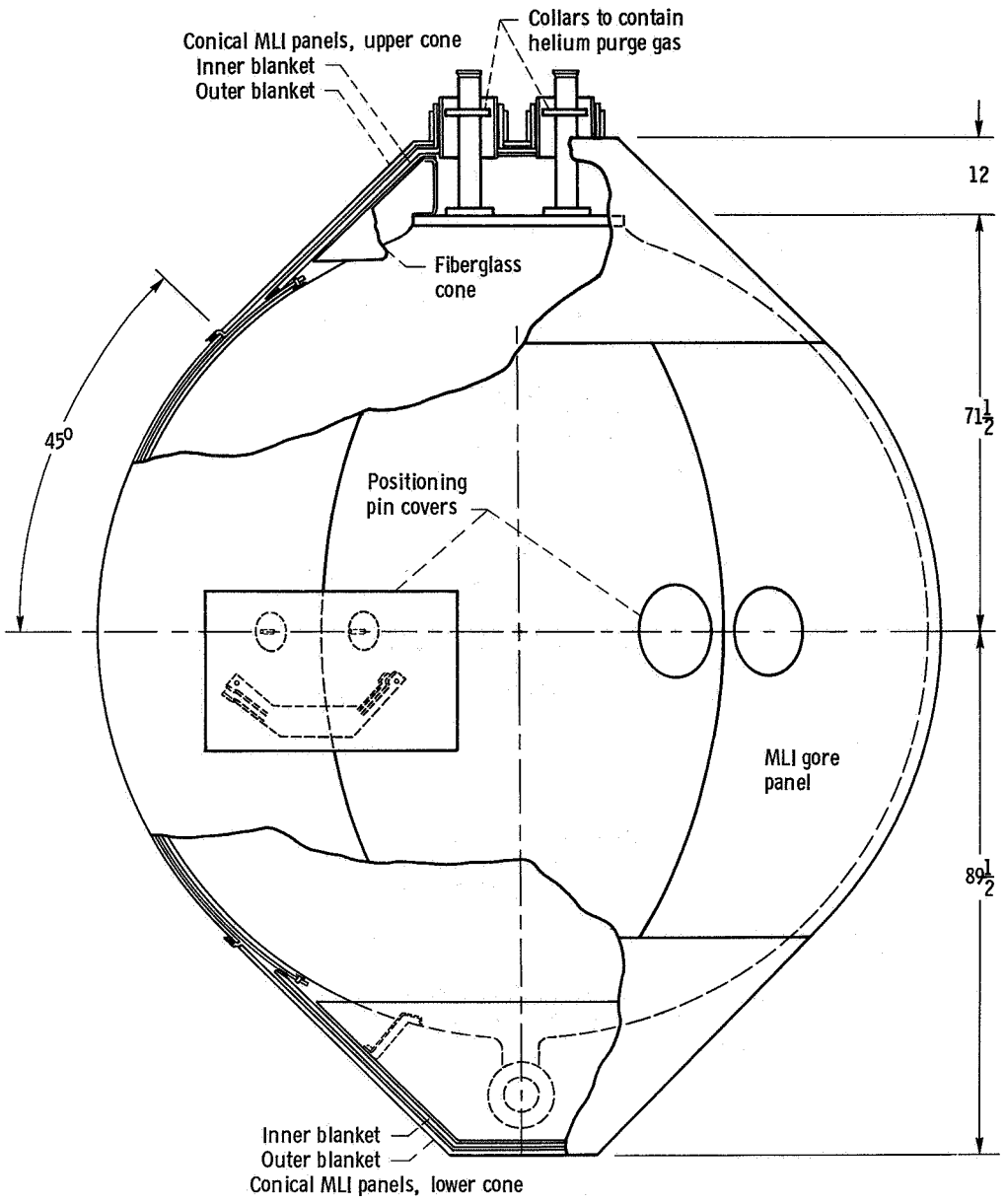

Figure 7. - Schematic of MLI system assembly. (All dimensions are in cm.)

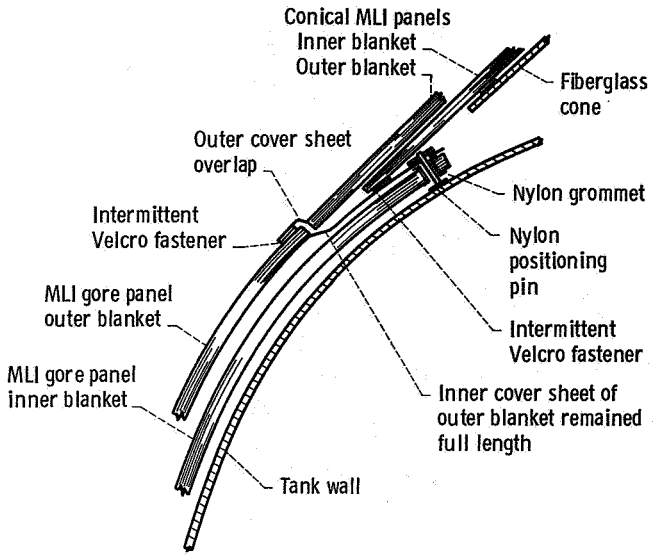

Figure 8. - Schematic of joints between MLI gore panels and conical MLI panels at top and bottom of tank.

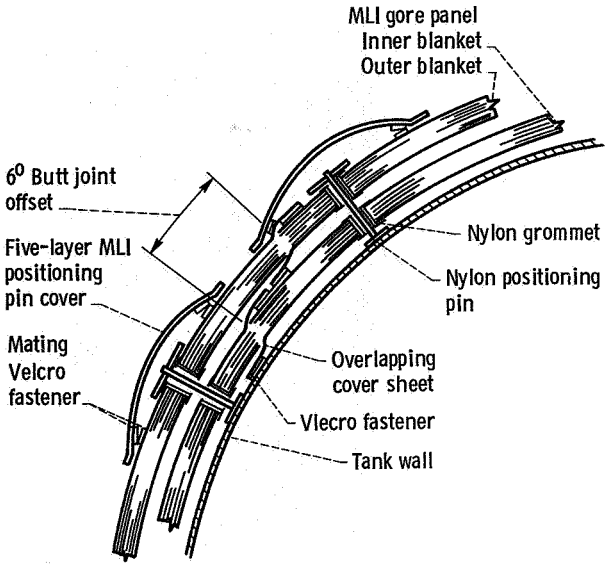

Figure 9. - Schematic of butt joint configuration between MLI gore panels showing overlapping cover sheets; shown in horizontal plane of tank equator with nylon positioning pins and five-layer MLI covers.

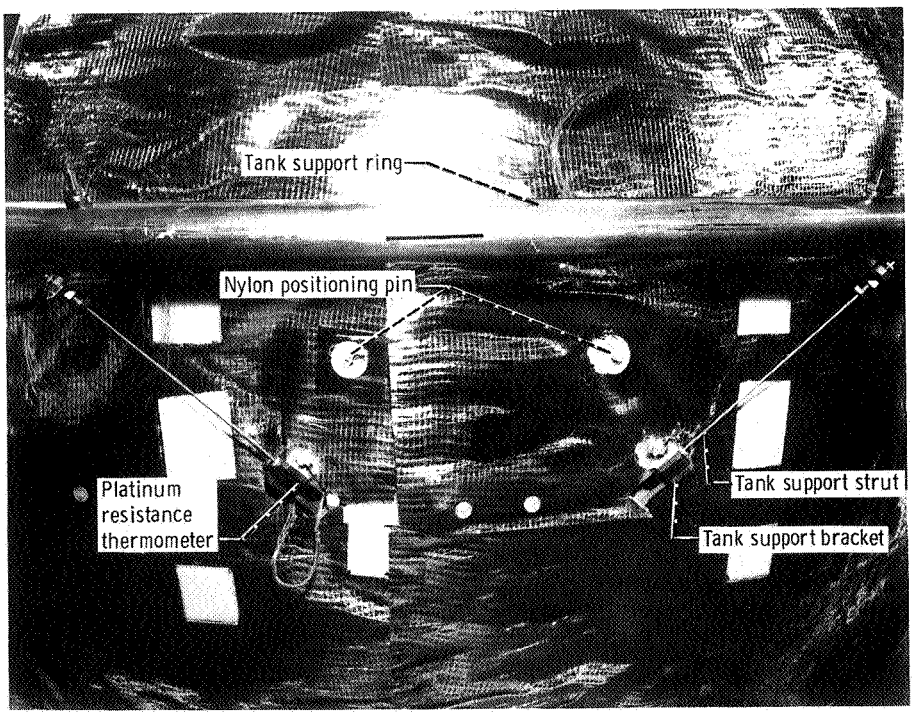

Figure 10. - Cutouts in MLI panels for tank support brackets.

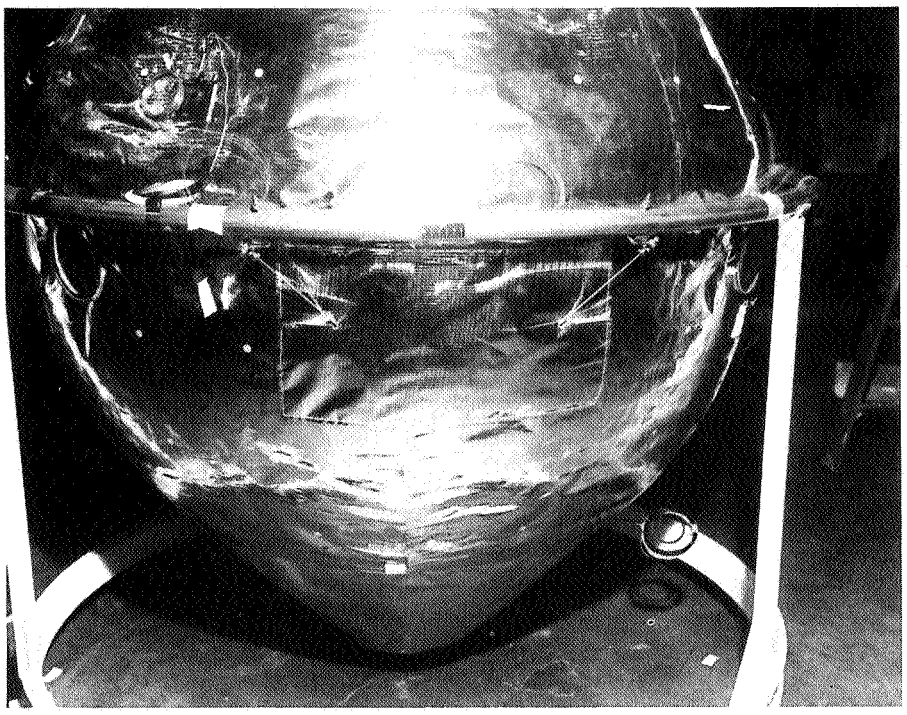

(a) Vicinity of tank support brackets.

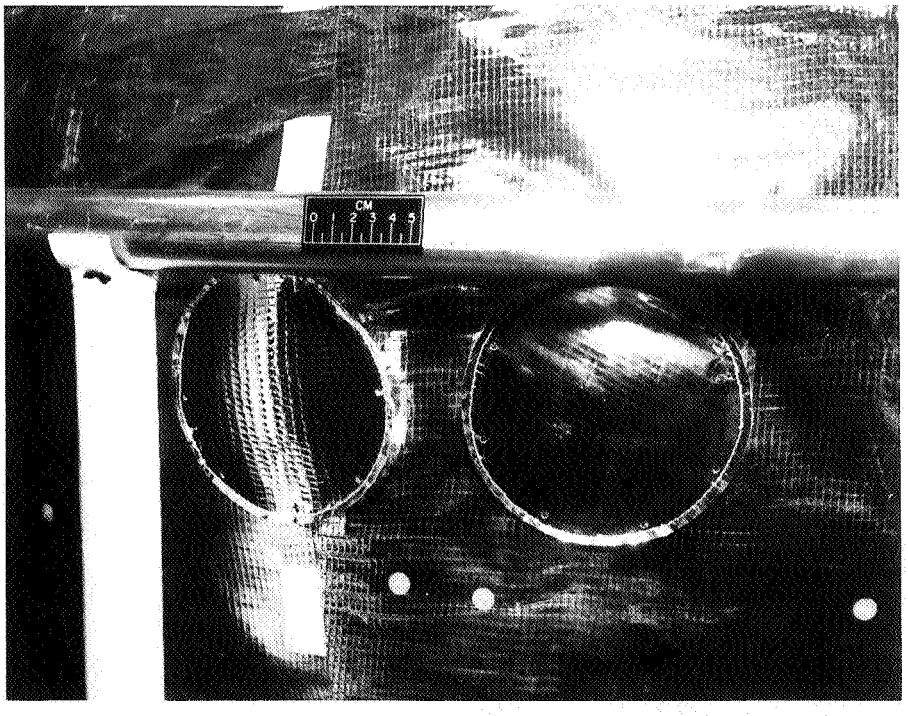

(b) For positioning pins only.

Figure 11. - Positioning pin covers.

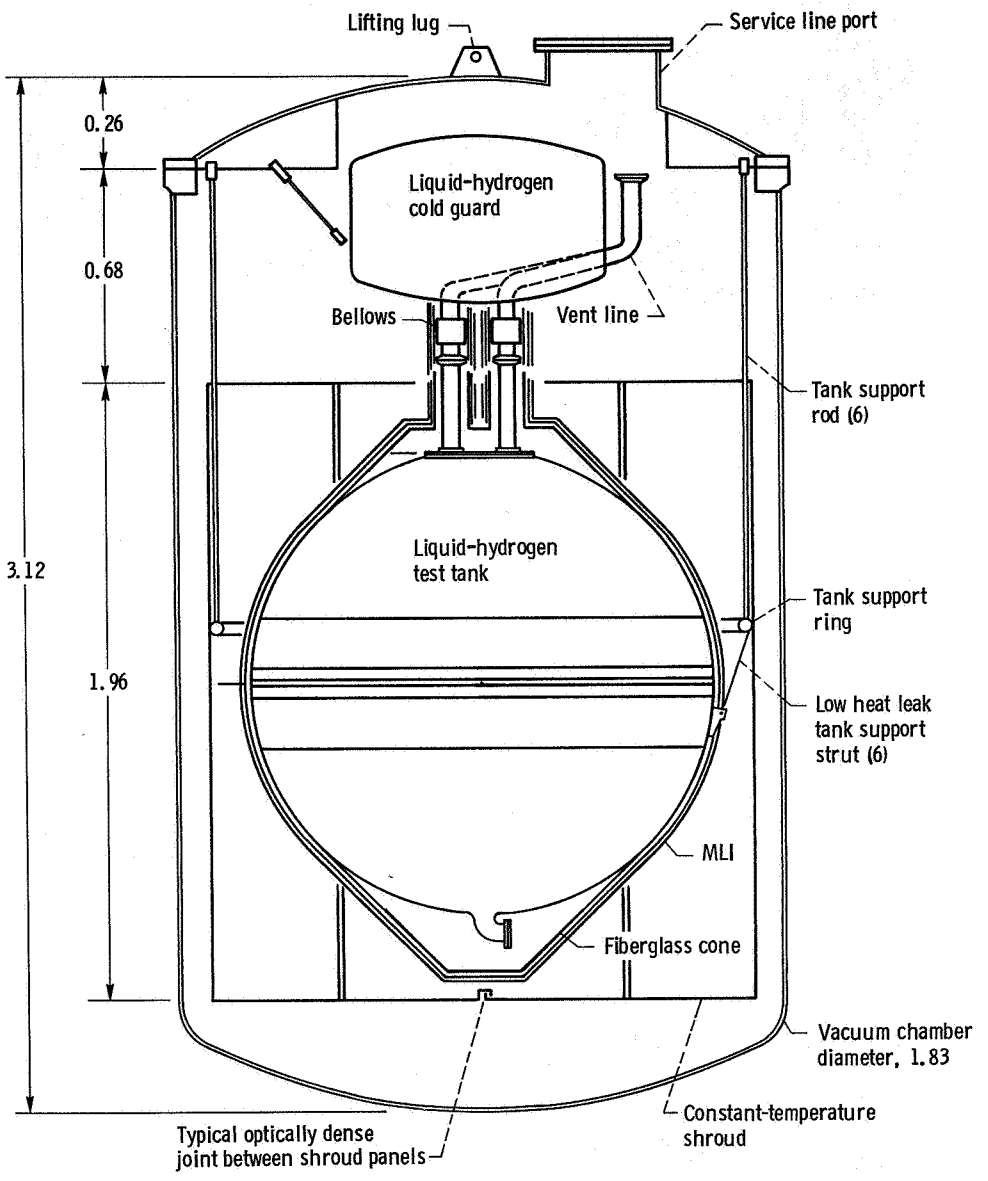

Figure 12. - Schematic showing installation of insulated test tank in vacuum chamber. (All dimensions are in cm.)

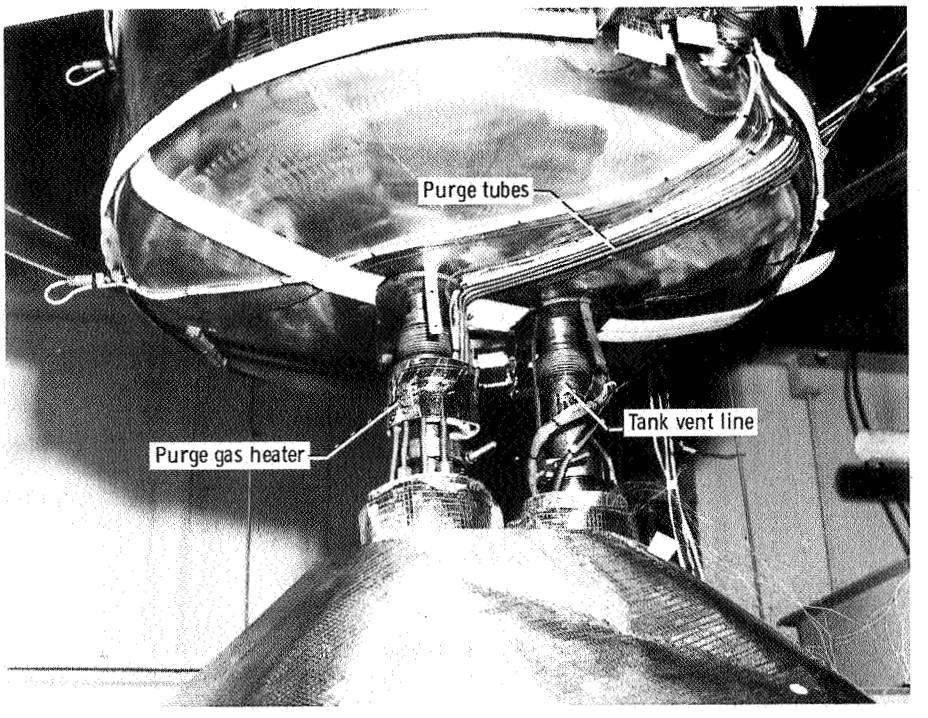

(a) Purge tubes brazed to bottom of cold guard.

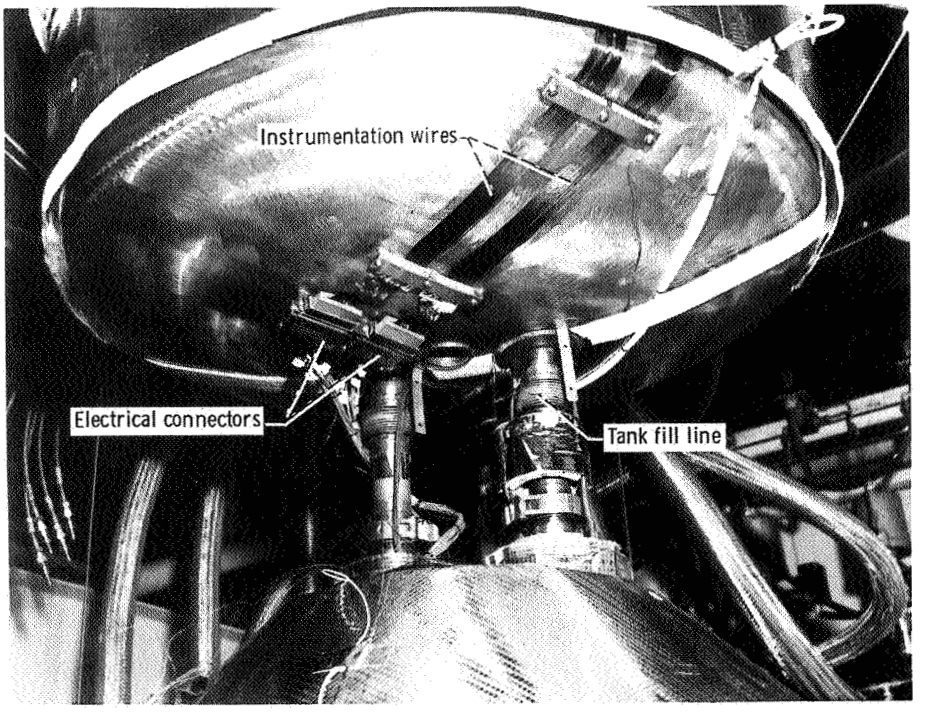

(b) Instrumentation wires adhesively bonded to bottom of cold guard.

Figure 13. - Cold guarding of purge tubes and instrumentation wires.

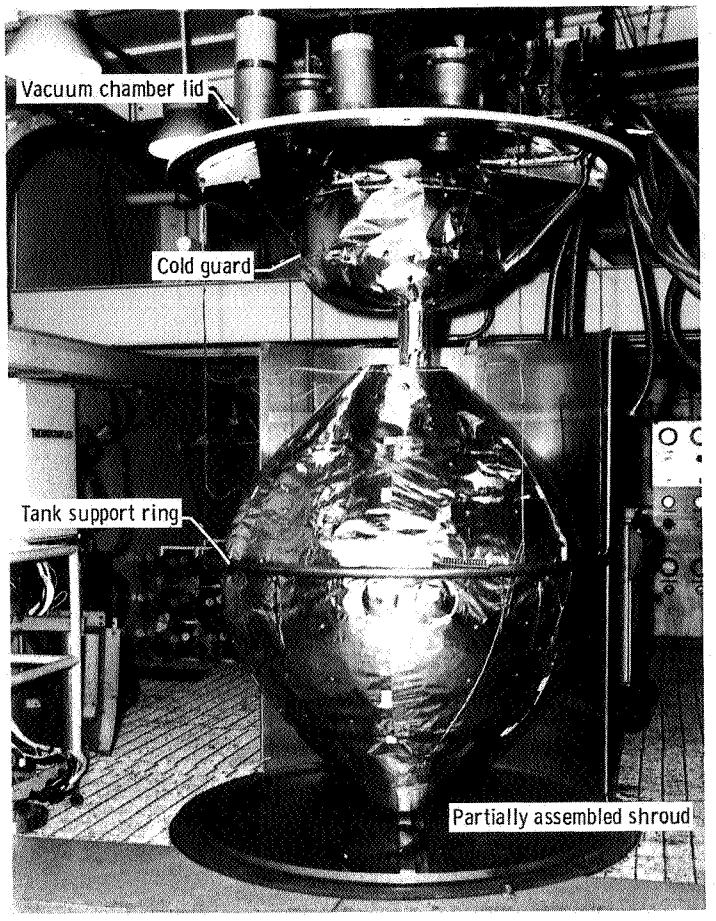

Figure 14. - Insulated test tank and cold guard.

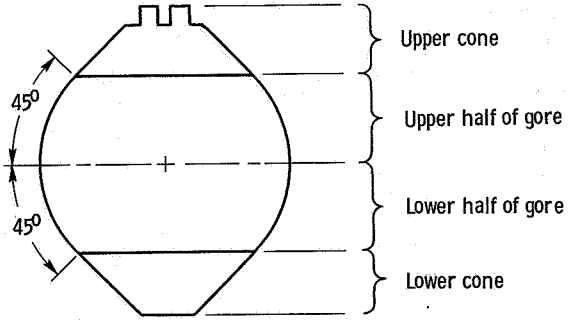

Four purge regions for insulation system

Purge region	Calculated volume		Calibrated volumetric flow[a], $d_o^2 C_d$	
	m^3	Percent of total	cm^2	Percent of total
Upper cone	0.0480	25.8	8.34×10^{-4}	27.3
Upper half of gore	.0433	23.3	6.84	22.4
Lower half of gore	.0433	23.3	6.86	22.5
Lower cone	.0515	27.7	8.47	27.8
Total	0.1861	100.1		100.0

[a]Orifice diameter, d_o, cm; discharge coefficient for choked flow, C_d.

Figure 15. - Purge regions and flow distribution for MLI.

Sampling tube pair	Symbol	Butt joint location		MLI panel location		
		MLI blanket	Relative to tank equator	MLI blanket	Relative to	
					Tank equator	Panel vertical centerline
1	○	Outer	45° above	Outer	----------	----------
2	△	Outer	22.5° above	Outer	22.5° above	On vertical centerline
3	□	Outer	22.5° above	Outer	22.5° above	On vertical centerline
4	▽	Inner	22.5° below	Inner	22.5° below	On vertical centerline
5	◇	Outer	22.5° below	Outer	22.5° below	On vertical centerline
6	◿	Outer	45° below	Outer	----------	----------

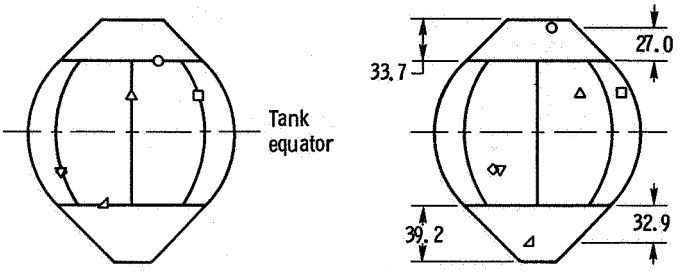

(a) Butt joint locations. (b) MLI panel locations.

Figure 16. - Location of sampling tubes where gas samples from within MLI system were obtained. (All dimensions are in cm unless noted otherwise.)

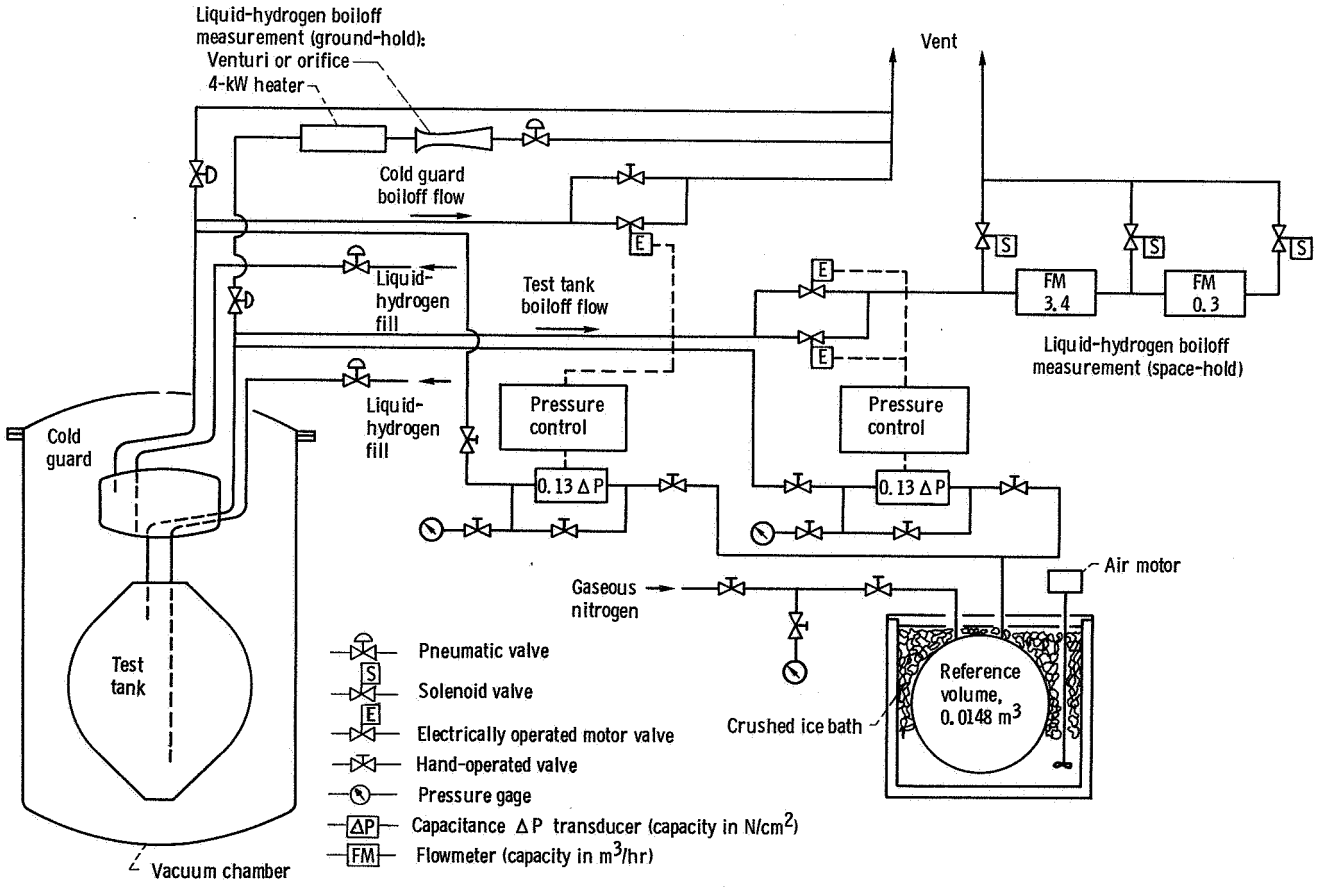

Figure 17. - Facility tank pressure control and boiloff measurement systems.

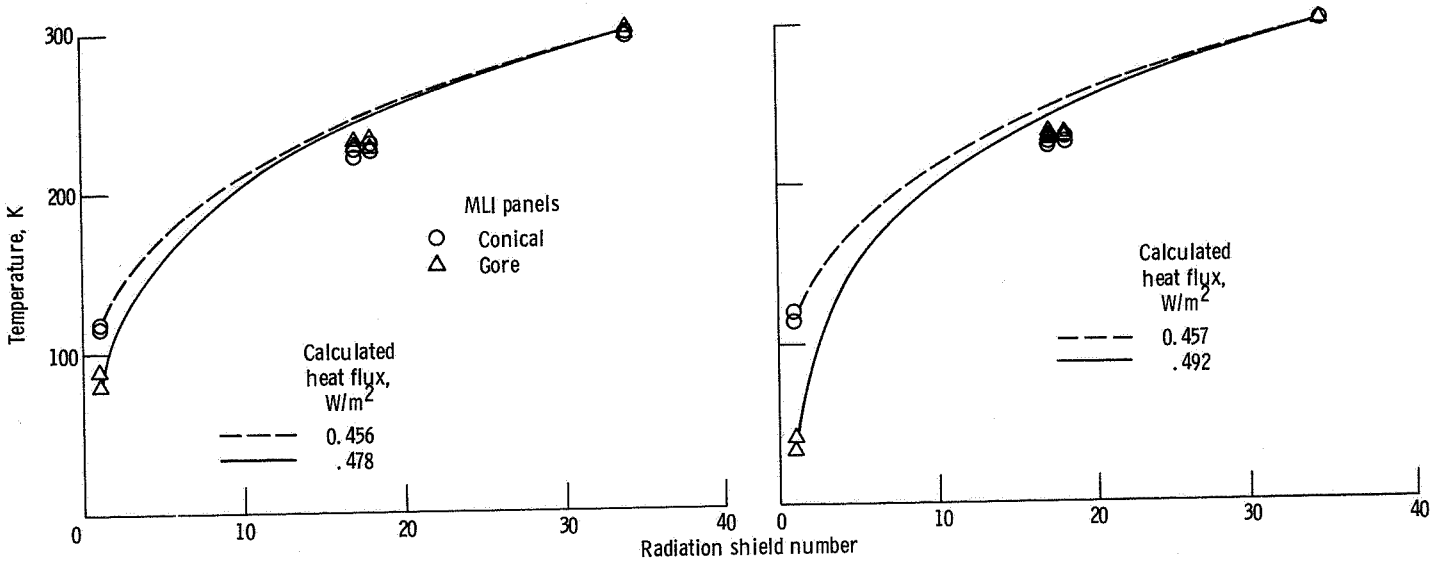

(a) Test 1.

(b) Test 7.

Figure 18. - MLI temperature profile for tests 1 and 7. Assumed layer density, LD, 17.7 layers per centimeter; emissivity, $\epsilon_{tot,\overline{h}}$, 0.050; interstitial pressure, IP, 3×10^{-4} newton per square meter (space-hold vacuum conditions).

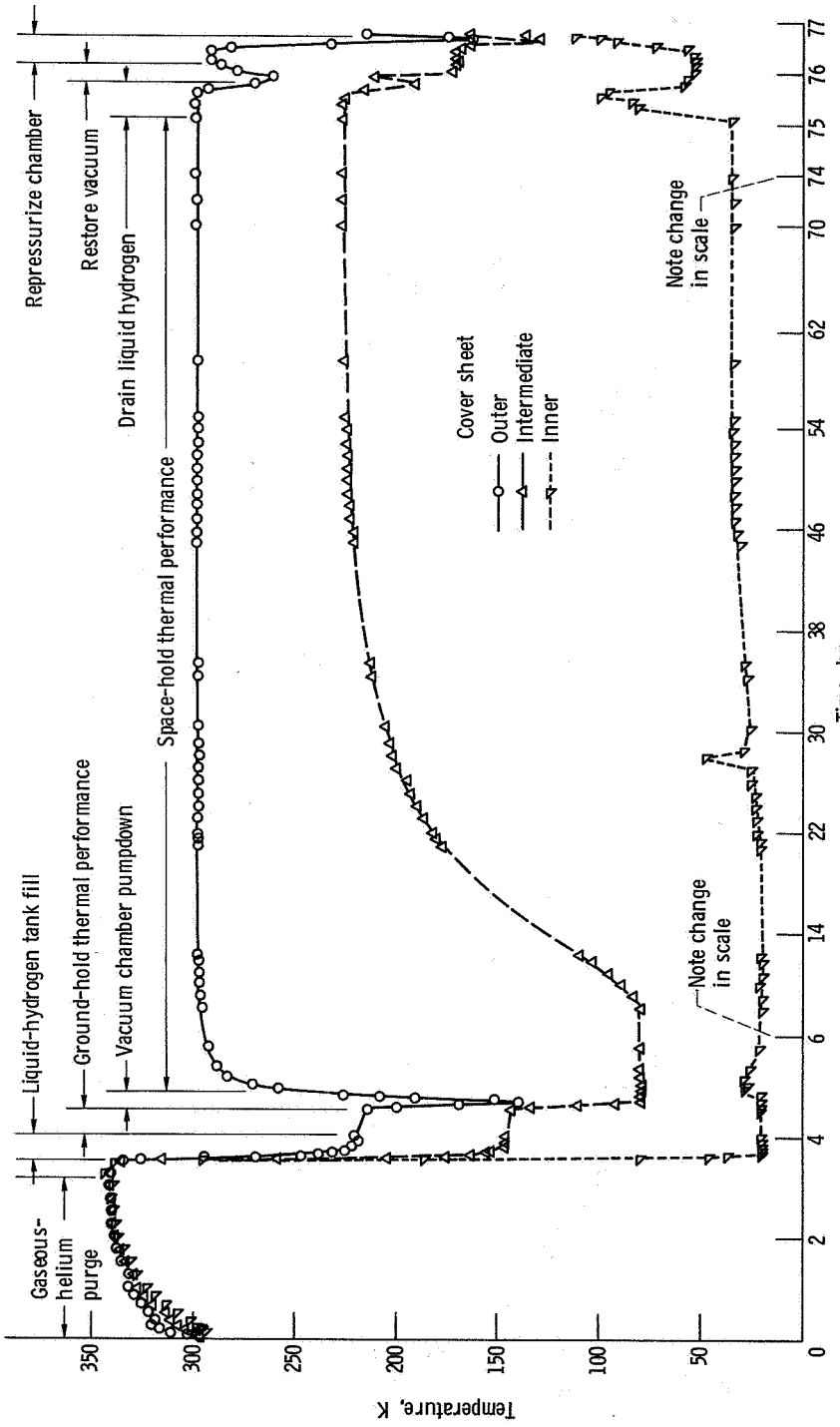

Figure 19. - MLI temperature history for lower gore panel (test 11-3).

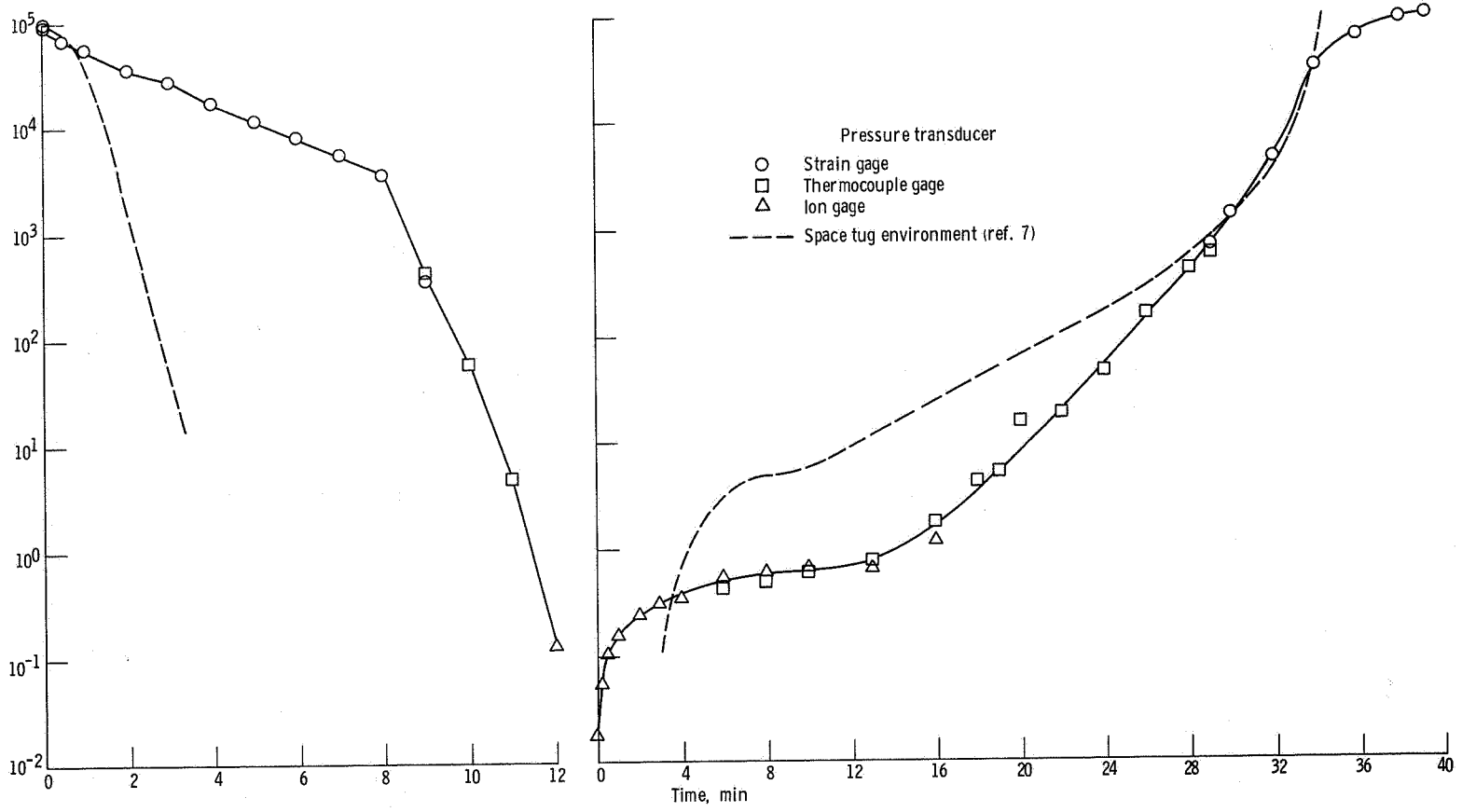

(a) Pumpdown.

(b) Repressurization.

Figure 20. - Vacuum chamber pressure history during pumpdown and repressurization (test 11-3).

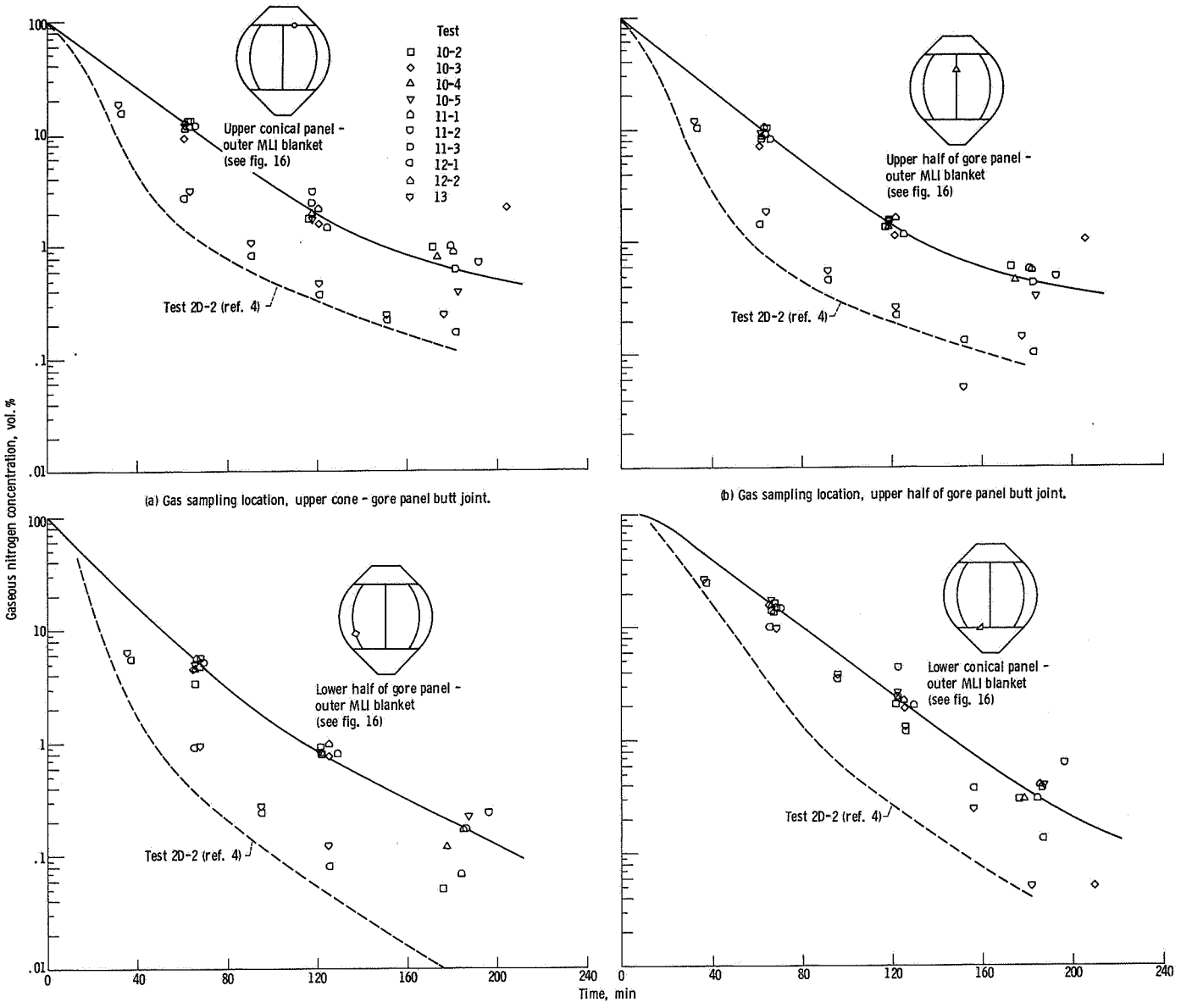

(a) Gas sampling location, upper cone - gore panel butt joint.

(b) Gas sampling location, upper half of gore panel butt joint.

(c) Gas sampling location, lower half of gore panel butt joint.

(d) Gas sampling location, lower cone - gore panel butt joint.

Figure 21. - Gaseous nitrogen concentration within MLI system. MLI system gaseous helium purge rate, 36 volumes per hour; vacuum chamber gaseous helium purge rate.

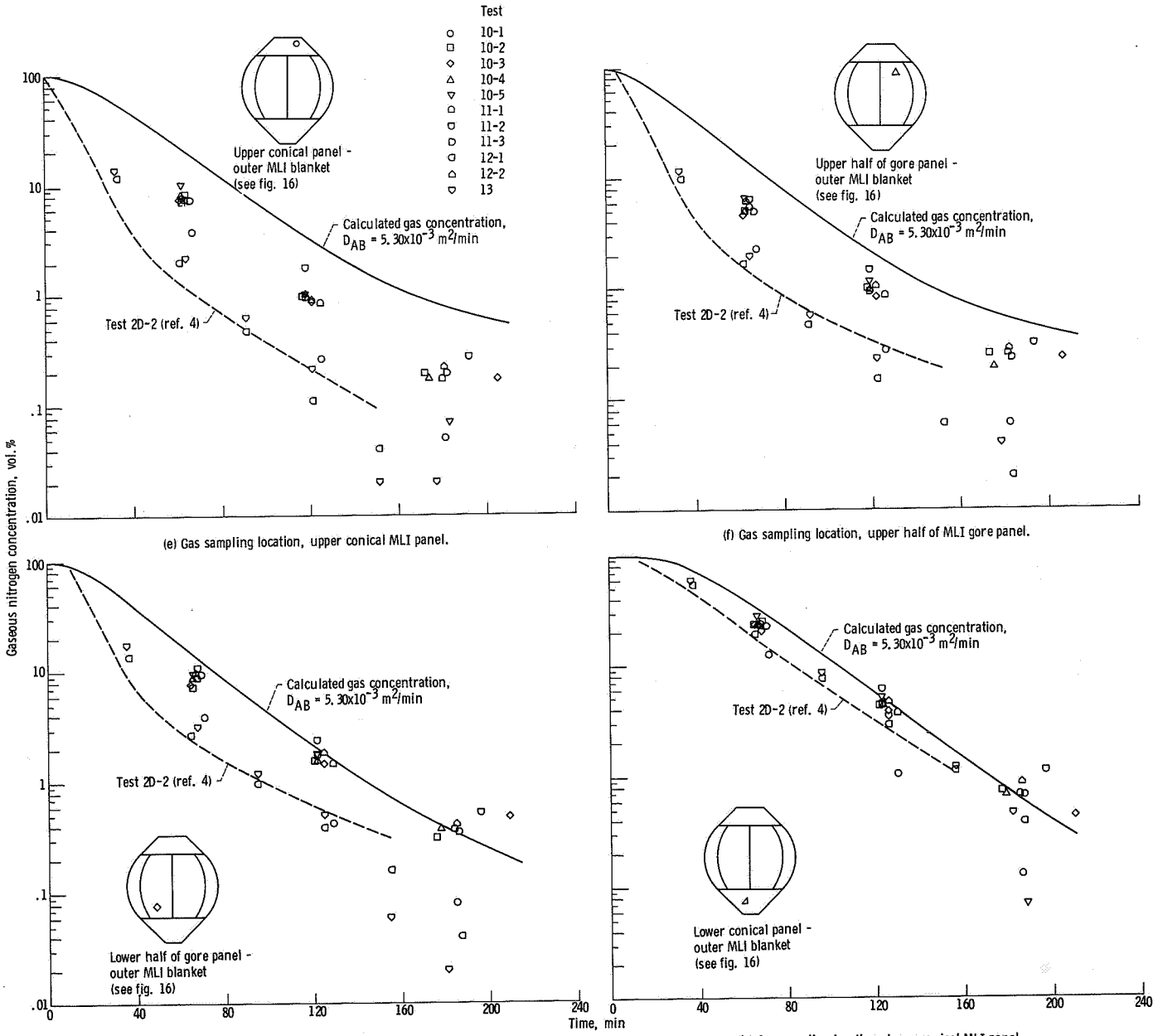

(e) Gas sampling location, upper conical MLI panel.

(f) Gas sampling location, upper half of MLI gore panel.

(g) Gas sampling location, lower half of MLI gore panel.

(h) Gas sampling location, lower conical MLI panel.

Figure 21. - Concluded.

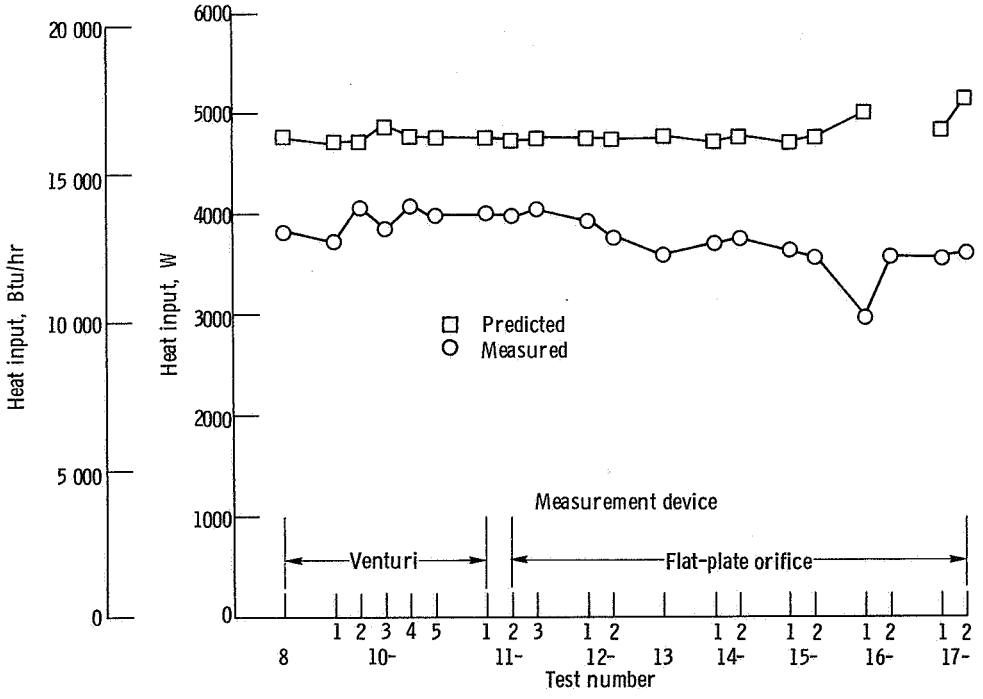

Figure 22. - MLI ground-hold thermal performance.

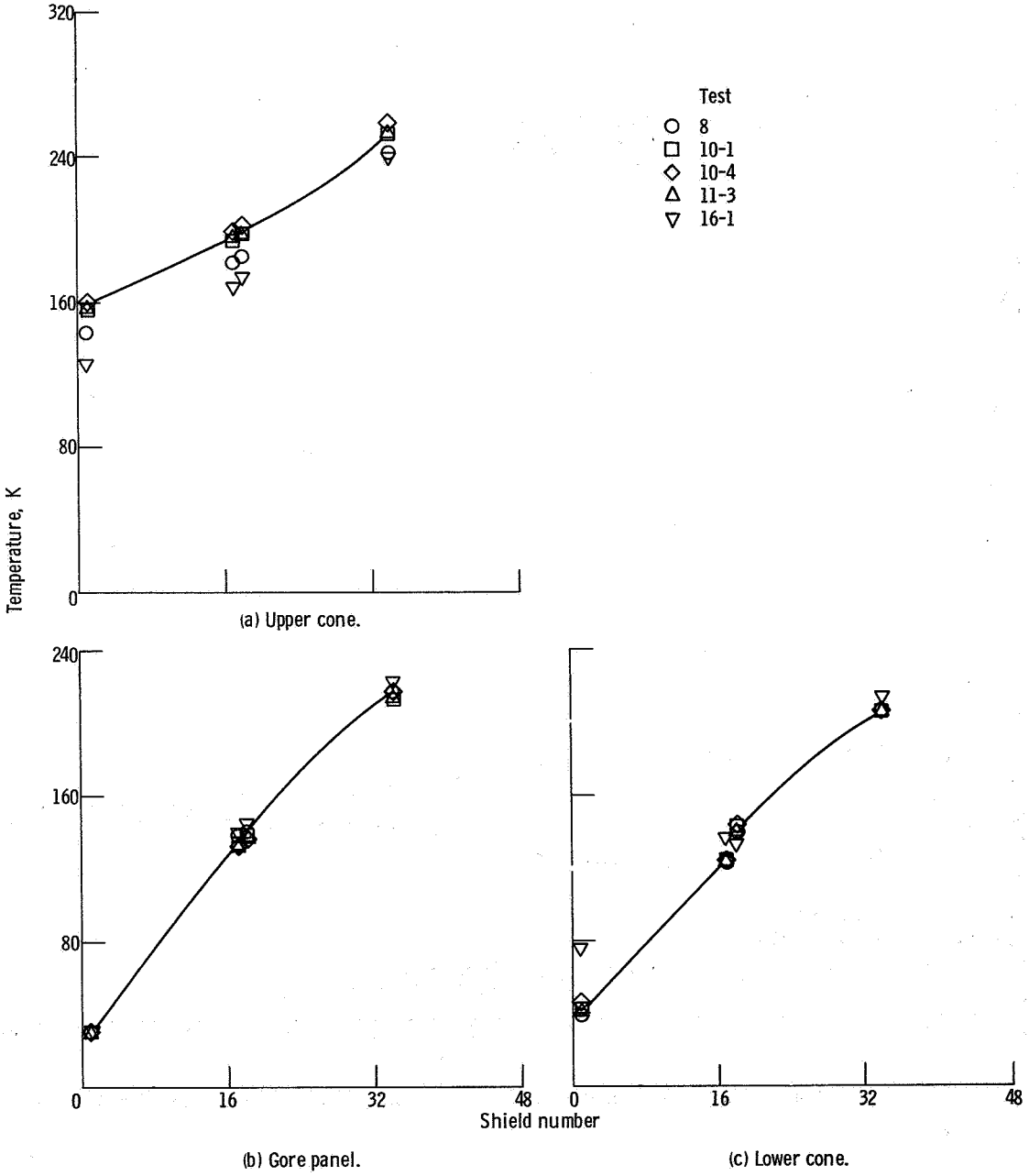

Figure 23. - MLI temperature profile (ground-hold conditions).

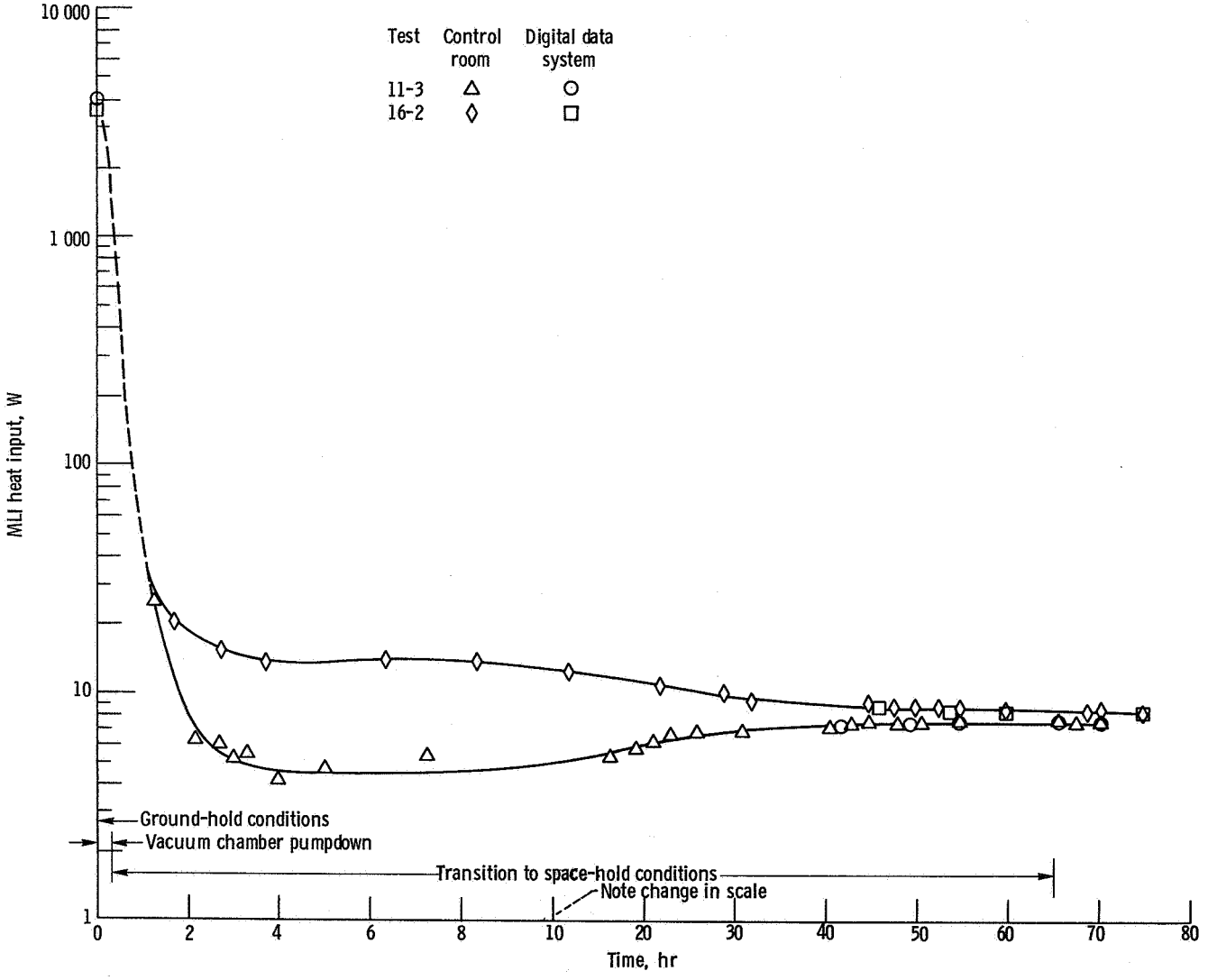

Figure 24. - History of heat input attributed to MLI during transition from ground-hold to space-hold conditions.

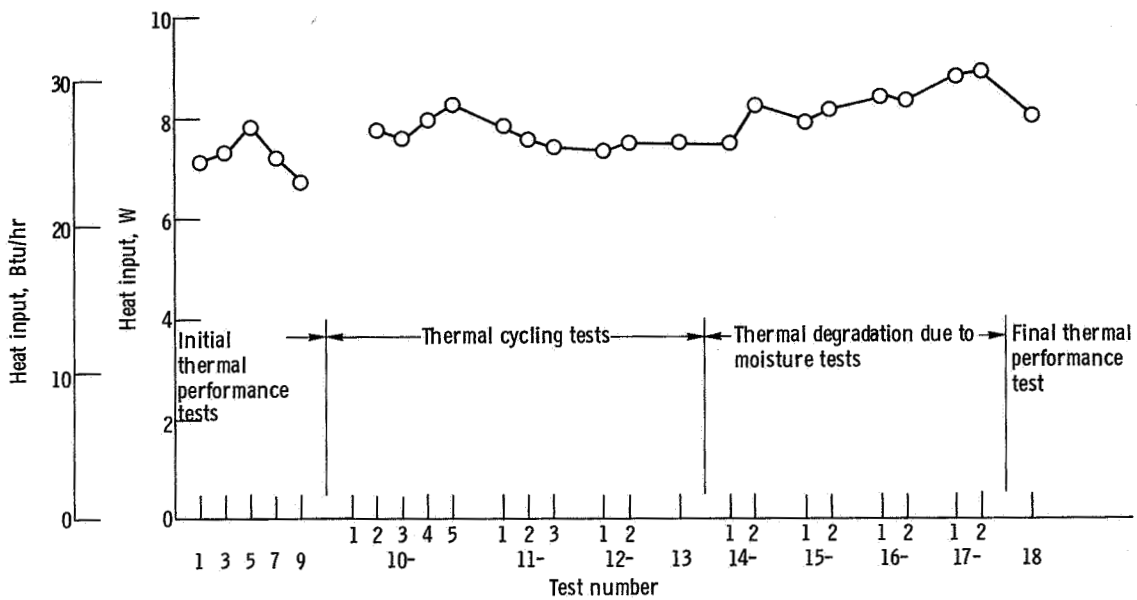

Figure 25. - MLI space-hold thermal performance.

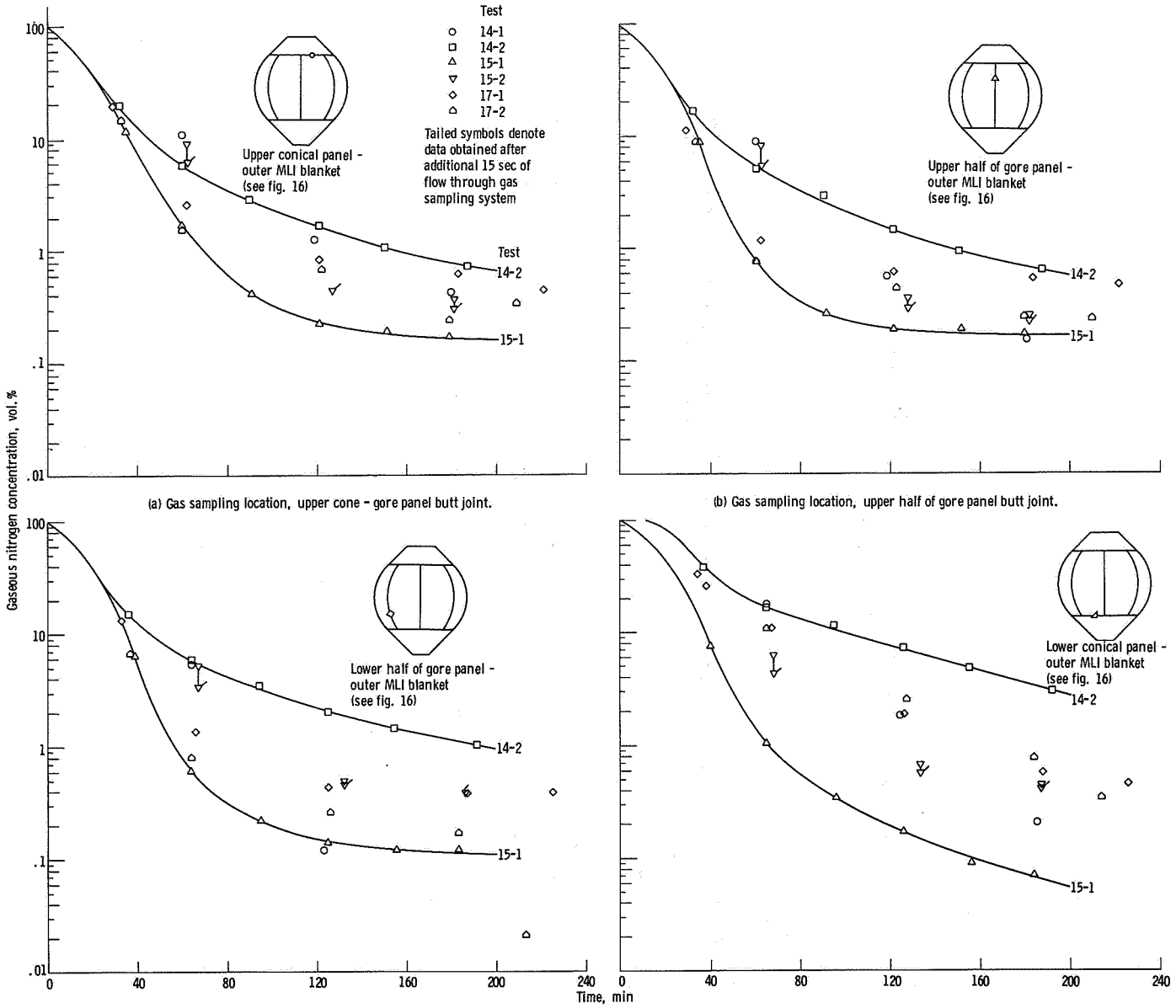

Figure 26. - Gaseous nitrogen concentration within MLI system. MLI system gaseous helium purge rate, 36 volumes per hour; vacuum chamber gaseous helium purge rate, 2.4 volumes per hour.

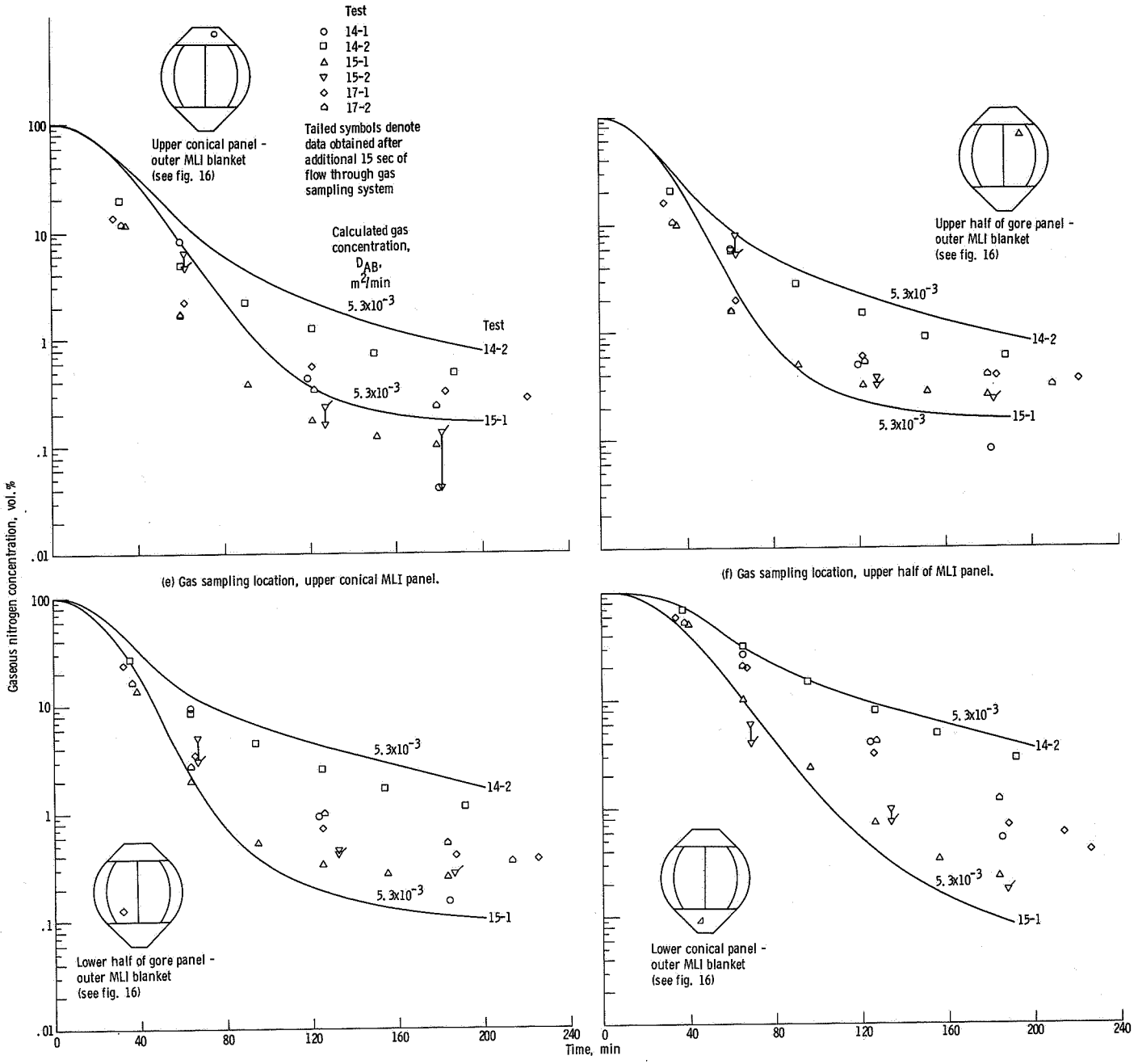

(e) Gas sampling location, upper conical MLI panel.

(f) Gas sampling location, upper half of MLI panel.

(g) Gas sampling location, lower half of MLI gore panel.

(h) Gas sampling location, lower conical MLI panel.

Figure 26. - Concluded.

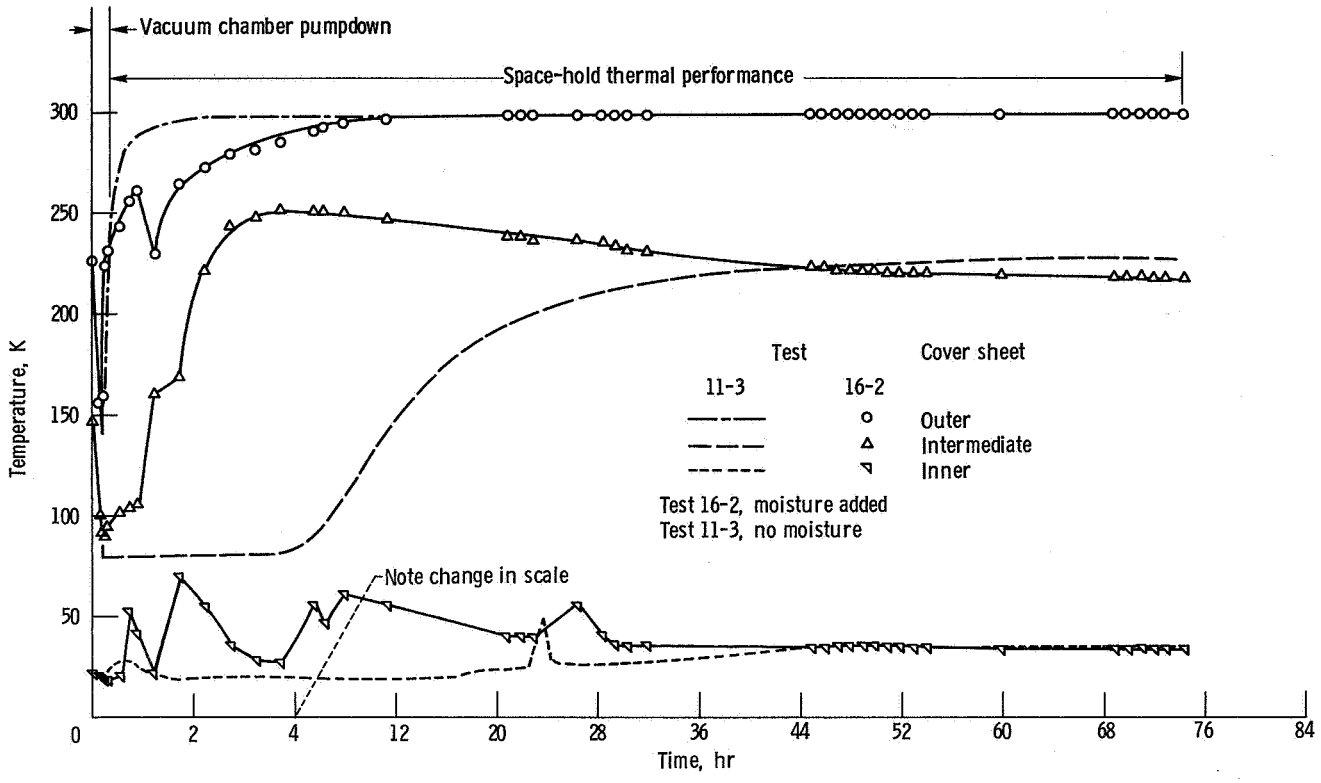

Figure 27. - Effect of moisture on MLI temperature history for lower gore panel (test 16-2).

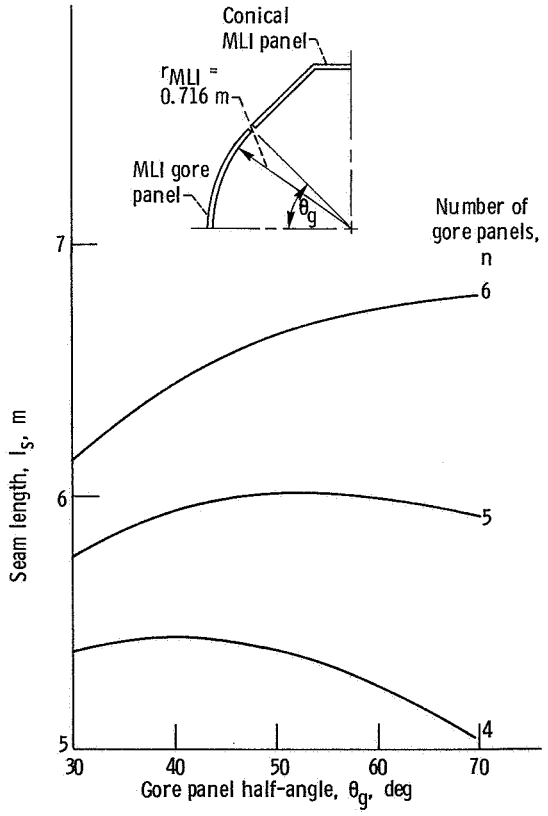

Figure 28. - Seam length for insulated spherical tank.

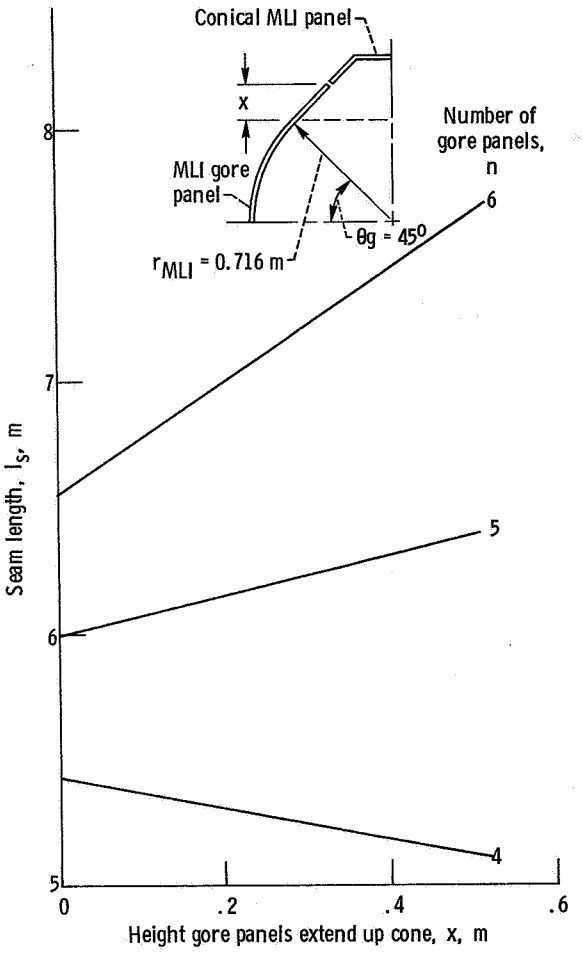

Figure 29. - Seam length for insulated spherical tank.

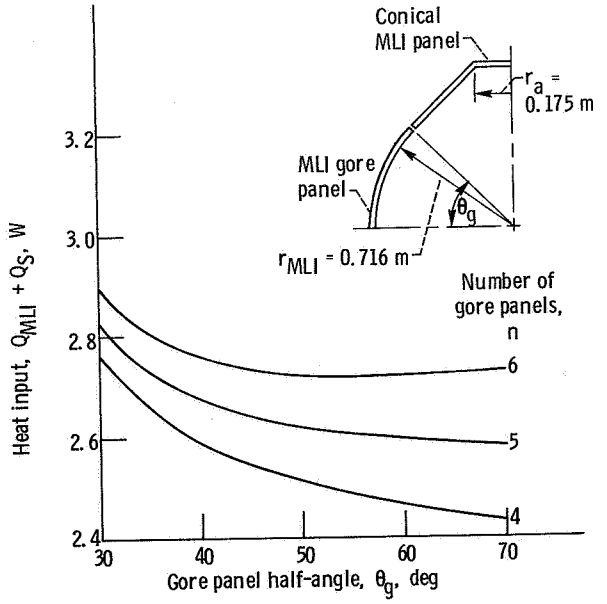

Figure 30. - Predicted heat input into upper half of test tank as function of gore panel half-angle and number of MLI gore panels.

1. Report No. NASA TP-1114	2. Government Accession No.	3. Recipient's Catalog No.
4. Title and Subtitle THERMAL PERFORMANCE OF GASEOUS-HELIUM-PURGED TANK-MOUNTED MULTILAYER INSULATION SYSTEM DURING GROUND-HOLD AND SPACE-HOLD THERMAL CYCLING AND EXPOSURE TO WATER VAPOR		5. Report Date August 1978 6. Performing Organization Code
7. Author(s) Irving E. Sumner		8. Performing Organization Report No. E-9443 10. Work Unit No. 506-21
9. Performing Organization Name and Address National Aeronautics and Space Administration Lewis Research Center Cleveland, Ohio 44135		11. Contract or Grant No. 13. Type of Report and Period Covered Technical Paper
12. Sponsoring Agency Name and Address National Aeronautics and Space Administration Washington, D. C. 20546		14. Sponsoring Agency Code

15. Supplementary Notes

16. Abstract

An experimental investigation was conducted to determine (1) the ground-hold and space-hold thermal performance of a multilayer insulation (MLI) system mounted on a spherical, liquid-hydrogen propellant tank and (2) the degradation to the space-hold thermal performance of the insulation system that resulted from both thermal cycling and exposure to moisture. The propellant tank had a diameter of 1.39 meters (4.57 ft). The MLI consisted of two blankets of insulation; each blanket contained 15 double-aluminized Mylar radiation shields separated by double silk net spacers. Nineteen tests simulating basic cryogenic spacecraft thermal (environmental) conditions were conducted. These tests typically included initial helium purge, liquid-hydrogen fill and ground-hold, ascent, space-hold, and repressurization. No significant degradation of the space-hold thermal performance due to thermal cycling was noted. Exposing the insulation to a 100-percent relative humidity environment for as long as 8 weeks resulted in increased heat transfer through the insulation system only 19 percent higher than the nominal space-hold thermal performance.

17. Key Words (Suggested by Author(s))

Multilayer insulation; Insulation thermal performance; Insulation purge; Cryogenic propellant storage; Spacecraft; Cryogens

18. Distribution Statement

Unclassified - unlimited
STAR Category 15

19. Security Classif. (of this report)	20. Security Classif. (of this page)	21. No. of Pages	22. Price*
Unclassified	Unclassified	72	A03

* For sale by the National Technical Information Service, Springfield, Virginia 22161

NASA-Langley, 1978